



Evaluación de la estabilidad del biochar: implicaciones para su uso en el secuestro de Carbono

Trabajo de Fin de Máster



Facultad de Química

Universidad de Sevilla

Curso 2015/2016

Autor: D. Mario Jesús Rosado Rodríguez

Director: D. José María de la Rosa Arranz

Co-directora: Dña. Heike Knicker

Instituto de Recursos Naturales y Agrobiología de Sevilla (IRNAS-CSIC)

Tutor: D. Alfonso Mazuelos Rojas

Facultad de Química; Universidad de Sevilla



Evaluation of the stability of biochar: implications for carbon sequestration in soils

Master Thesis



Faculty of Chemistry

University of Seville

Academic course 2015/2016

Autor: D. Mario Jesús Rosado Rodríguez

Director: D. José María de la Rosa Arranz

Co-directora: Dña. Heike Knicker

Instituto de Recursos Naturales y Agrobiología de Sevilla (IRNAS-CSIC)

Tutor: D. Alfonso Mazuelos Rojas

Facultad de Química; Universidad de Sevilla

Máster en Estudios Avanzados en Química
(Master Thesis)

Evaluation of the stability of biochar:
Implications for carbon sequestration in soils

Supervisor

Co-supervisor

Dr. D. José M^a De la Rosa Arranz
IRNAS-CSIC

Prof. Dña. Heike Knicker
IRNAS-CSIC

Tutor

Dr. D. Alfonso Mazuelos Rojas
Profesor titular de la Universidad de Sevilla
Departamento de Ingeniería Química

Sevilla, 8th of September 2016.

INDEX

AGRADECIMIENTOS/ACKNOWLEDGEMENTS	4
List of abbreviations and achronyms used	5
1. ABSTRACT	6
2. INTRODUCTION	7
2.1. Feedstock, pyrolysis process and biochar production	8
2.2. Physical and chemical properties of biochars	9
2.2.1. <i>Physical properties</i>	9
2.2.2. <i>Chemical properties</i>	10
2.3. Evolution of biochar in soil.....	11
2.3.1. <i>Physical alteration</i>	11
2.3.1.1. <i>Fragmentation to smaller particle size</i>	11
2.3.1.2. <i>Heteroaggregation with other soil particles</i>	11
2.3.2. <i>Chemical alteration</i>	12
2.3.3. <i>Persistence of biochar in soil</i>	13
2.4. Potential of biochar as sink of carbon in soils.....	14
3. OBJECTIVES.....	16
4. MATERIALS AND METHODS.....	18
4.1. Experimental desing of the field experiment with biochar amended soils	18
4.2. Biochar sampling.....	18
4.2.1. Description of biochar samples	19
4.2.2. Sampling procedure	19
4.3. Methodology	20
4.3.1. Physicochemical analysis.....	20
4.3.1.1. <i>Micro-elemental analysis (C,N)</i>	20
4.3.1.2. <i>pH and electrical coductivity</i>	21
4.3.1.3. <i>Biochar fragmentation</i>	21
4.3.2. Fourier Transform Infrared spectroscopy (FT-IR).....	21
4.3.2.1. <i>Theoretical fundaments for application of FT-IR spectroscopy</i> <i>in soils</i>	21
4.3.2.2. <i>Applied conditions for FT-IR spectroscopy</i>	22
4.3.3. ¹³ C solid-state Nuclear Magnetic Resonance Spectroscopy	22
4.3.3.2. <i>Theoretical fundaments for application of NMR spectroscopy in soil</i> ...	22
4.3.3.2. <i>Applied conditions for ¹³C NMR experiments of biochar samples</i>	23
4.3.4. C stabilization in biochar by using a respiration experiment (Respicond)	23

4.3.4.1. <i>Theoretical fundamentals of Respirometer Respicond®</i>	23
4.3.4.2. <i>Conditions for the experiment</i>	24
4.3.4. Field Emission Scanning Electron Microscopy (FESEM)	25
4.3.4. <i>Applied conditions for FESEM</i>	25
5. RESULTS AND DISCUSSION	26
5.1. Analytical characterization of biochars and soil.....	26
5.1.1. <i>Macro-elemental composition of original biochars</i>	26
5.1.2. <i>Macro-elemental composition of aged biochars</i>	27
5.2. Physical characterization.....	28
5.2.1. <i>Fragmentation</i>	28
5.2.2. <i>pH and electrical conductivity (EC)</i>	29
5.3. Elemental composition of biochars	29
5.4. FT-IR spectroscopy	32
5.4.1. <i>FT-IR of initial biochars</i>	32
5.4.2. <i>FT-IR of aged biochars (24 months)</i>	33
5.5. ¹³ C Solid-State NMR spectroscopy	36
5.2.1. ¹³ C NMR spectra of initial biochars (<i>t₀</i>)	36
5.2.2. ¹³ C NMR spectra of aged biochars (<i>t₂</i>)	37
5.6. Field Emission Scanning Electronic Microscopy (FESEM).....	40
5.7. Carbon stability of biochars (respiration experiment).....	41
6. CONCLUSIONS	45
7. REFERENCES	46

AGRADECIMIENTOS/ACKNOWLEDGEMENTS

A todo el grupo de investigación de Materia Orgánica en Suelos (MOSS) del Instituto de Recursos Naturales de Sevilla (IRNAS-CSIC), en especial a D. José María De la Rosa Arranz y Dña. Heike Knicker, por trasnmitirme su vocación, energías y entusiasmo por la investigación; a Dña. Marina Paneque Carmona, por el apoyo y todo lo que me ha enseñado durante estos meses de Trabajo. Por supuesto a Marta, María, Alba y Nicasio por los consejos y explicarme las dudas que han surgido por el camino. A Dña. Ana Miller, del grupo de investigación de Agroquímica, microbiología ambiental y conservación de suelos, por el apoyo y la ayuda ofrecida en la sección de microscopía del presente trabajo. Y como no, a mi tutor, D. Alfonso Mazuelos Rojas, por su disposición y apoyo.

Por otro lado, también quisiera agradecer la ayuda ofrecida a D. Javier Navas Pineda del Departamento de Química Física de la Universidad de Cádiz, por haberme cedido amablemente el equipo de su departamento en el momento más crítico de la investigación.

A mi familia, por ellos soy lo que soy. Para mis padres por sus consejos, comprensión, amor y ayuda en los momentos más difíciles. Por haberme dado todo lo que soy como persona, mis valores, principios, carácter, empeño y coraje para lograr mis objetivos.

Gracias.

List of abbreviations and achronyms used

ABBREVIATIONS AND ACHRONYMS	
CEC	Cation exchange capacity
EC	Electrical conductivity
CPMAS	Cross-Polarization Magic Angle Spinning
CWB	Certified wood biochar (sample)
GHGs	Greenhouse gases
KWB	Kiln-wood biochar (sample)
NOM	Natural organic material
OC	Organic carbon
OM	Organic matter
PAHs	Polycyclic aromatic hidrocarbons
PCM	Pyrogenic carbon matter
PSB	Paper sludge biochar
PyC	Pyrogenic carbon
PyOM	Pyrogenic organic matter
PWB	Pine wood biochar
PZNPC	Point of zero net point charge
SOC	Soil organic carbon
SOM	Soil organic matter
SSB	Sewage sludge biochar
TC	Total carbon
TOC	Total organic carbon
VOCs	Volatile organic compounds
VM	Volatile matter
WHC	Water holding capacity

1. ABSTRACT

Biochar is the byproduct obtained by the pyrolysis biomass, which generally has a high porosity and high content in organic carbon. From an agronomical point of view, numerous studies have shown that biochar may improve physical properties and soil quality, thus biochar could act as soil ameliorant. On the other hand, biochar has a great potential to mitigate the emissions of carbon dioxide (CO₂) to the atmosphere. This is due to biochar is rich in recalcitrant carbon, which is more stable than the original biomass, thus biochar could be used as an effective carbon sink in soils.

Several factors such as the feedstock and pyrolysis conditions will determine the composition, structure and properties of biochar. In addition, little is known concerning how degradation affects biochar. Beside this, it is of vital interest to develop a safe strategy to reduce the net balance of CO₂ emissions, thus it is important to know how degradation and aging at field conditions will affect the composition and C stability of biochars once they are incorporated to soil.

With these objectives, the present Master Thesis analyzed five different types of biochar, which were subjected to an “aging” process under Mediterranean climate conditions and to a respiration experiment under controlled conditions. For the field experiment, biochars were mixed with a calcic cambisol in the experimental farm “La Hampa” (Coria del Río, Seville). Seeds of sunflower plants (*Helianthus annuus*) were planted and harvested after 5 months. After 6, 12 and 24 months of incubation at field, soil samples were taken and biochar particles were carefully separated by hand.

Biochar alterations were assessed by measuring its elemental composition (C, N contents) pH, electrical conductivity (EC) and fragmentation degree. Other analytical tools, such as Fourier Transformation InfraRed Spectroscopy (FT-IR) and ¹³C Solid State Nuclear Magnetic Resonance (NMR) were applied to detect changes in the the functional groups of biochars.

The characterization of biochars showed their heterogeneity, which is attributed to their different nature and pyrolysis conditions. After 24 months at field under Mediterranean climate conditions, biochars exhibited a clear decrease in the OC content and aromaticity (measured by ¹³C NMR spectroscopy). On the contrary, alkyl and carboxyl-C increased. FESEM results confirmed the heterogeneity of biochars, the presence of microbiota and the collapse of biochar structures and pores with ageing.

Respiration experiments under controlled conditions (respicond experiment) showed that the biochars tested are less recalcitrant than previously stated assumed by other authors. Pine wood biochar (PWB) and kiln-wood biochars (KWB) were more stable than the other biochars under Mediterranean climate conditions, which mean residence time of the C from the stable pool (MRT₂) approximately four to five times greater than the MRT₂ of the bulk cambisol.

2. INTRODUCTION

Biochar is a porous and high-carbon content material, resultant from the pyrolysis process which consists on heating biomass or organic residues over 250°C in the absence of oxygen. Biochar is produced as a byproduct of the pyrolysis process with the main goal to be used as a soil amendment (De la Rosa et al., 2014). The appearance of biochar is similar to charcoal and activated carbon but the main difference among them is their use. Charcoal is mainly used as source of energy, while biochar is used as soil amendment. Biochar has been also proposed as an efficient tool for carbon sequestration (De la Rosa et al., 2014). It offers a sustainable tool for agriculture management and producing added-value products and reducing contaminant residues.

Because of the growth in intensive agriculture and the exponential increase of population, with the consequent rise of waste generated, biochar is an important weapon to combat the possible environmental impacts derived. In addition, biochar offers a new coordinated, economic and ecological agriculture way to achieve human requirements (Mao et al., 2012). Its application is particularly important in arid and semiarid agricultural areas as Mediterranean countries, due to factors as water storage, overgrazing, intense agriculture and fire frequency (De la Rosa et al., 2014). For this reason biochar could be used as a new ecological amendment which may enhance quality and plant growth (Knicker, 2014), it also has as advantage that the OM of biochars is more stable than the original OM from biomass residues. However, it requires an understanding of relations among composition, structure and stability to contribute to soil fertility. It has been shown evidences of black carbon in soils, with high aromaticity, practically at all climate zones, but there are little studies that treat chemical structure of char residues, being scarce in those that treat changes with time (Knicker, 2007).

In recent years, there are detailed studies and publications describing short-term effects of biochars focused on (sub)tropical regions (Jien et al., 2015). However, there is a lack of knowledge in which concern the real carbon sequestration potential and stability of biochar, rather aging effect, under Mediterranean climate conditions. Thus, the present work discusses the alterations on the physicochemical properties of different biochars due to the aging under Mediterranean climate conditions. In order to achieve this goal, a typical agricultural soil from south west Spain (a calcic *cambisol*) was amended with five different biochars, which were hand-picked from the amended soils during two years. It also was carry on a respirometer experiment with a mix of biochar sample and soil.



Figure 1. View of a sewage sludge biochar produced by pyrolysis at 500 °C

2.1. Feedstock, pyrolysis process and biochar production

Pyrolysis is a physicochemical decomposition process of organic matter (OM) by heat action and oxygen absence, similar to the technology used in the bioenergy industries. The final products of a pyrolysis process are a solid fraction rich in C (usually called 'biochar'), a heavy liquid fraction (usually called 'bio-oil') and a gaseous fraction (called 'syngas', which mainly consists of CH₄, CO and CO₂).

Table 1. Initial feedstock mass fate between products of pyrolysis processes (IEA, 2007; Brown, 2009; Funke & Ziegler, 2010; Schulze et al., 2016)

Process	Reaction conditions	Liquid (bio-oil)	Solid (biochar)	Gas (syngas)
Fast Pyrolysis	Moderate temperature (~450°C) Short-residence time (<2 s)	75% (25% water)	12%	13%
Intermediate Pyrolysis	Low-moderate temperature (~500 °C) Moderate residence time (~10-20 s)	50% (50% water)	25%	25%
Slow Pyrolysis	Low-moderate temperature Long residence time (~5-30 min)	30% (70% water)	35%	35%
Gasification	High temperature ~800°C Moderate residence time (~10-20 s)	10% (80% water)	5%	85%
Hydrothermal carbonization	Low-moderate temperature (~280-250°C). No vapour residence time. Processing time (Moderate residence time (~1-12 h)	50-80% (50-30% water)	5-20%	2-5%

There are multiple factors that cause changes in the physicochemical properties of biochar such as pyrolysis type (and their reactions) and initial feedstocks (Kan et al., 2016). However, not all kind of feedstock or pyrolysis conditions are suitable for biochar production. The chemical and physical properties derived from the original feedstock submitted to pyrolysis are well-known (Chia et al., 2012). The reactions occasioned during the pyrolyzation are dehydration, decarboxylation, dehydrogenation, oxidation from saturated to unsaturated hydrocarbons and methylation (Knicker, 2007; Knicker, 2011). The result of these reactions cause a condensation forming polycyclic aromatic structures depleted of H and O in solid phase. However, during the pyrolysis parameters such as pressure, temperature or time will also affect the physicochemical properties of biochar. The initial structure of feedstock is similar to the resulting biochar, especially for feedstock containing high composition in cellulose (Sohi et al., 2010).

The choice of the right feedstock to be subjected to pyrolysis process is determined by their purpose so it has to be chosen carefully, rather, a wide range of possibilities for wastes is used for production of biochar. Organic wastes are common feedstocks for biochar generation (Kwapinski et al., 2010), but it omphrehends from biomass to manures or other animal wastes as agricultural and forestry residues, human waste, sewage sludge,

municipal solid waste, wood, straw or hazelnut and peanut shells. Whereupon, the source of origin of the feedstock for biochar production determines the macromolecules that constitute biochar or even composition may have similar content although different proportions and/or structures. This fact is determinant for high temperature exposure. An illustrative example is that formed by cellulose, hemicellulose and lignin. These three compounds have polysaccharides in their structures but lignin is more resistant to thermal decomposition, accordingly lignin-rich compounds produce the highest biochar yields (Triphati et al., 2016).

2.2. Physical and chemical properties of biochars

The characteristics of biochar, potential uses and quality are determined by multiple factors, as previously mentioned, they are mainly, the type of feedstock used and the pyrolysis conditions (Demirbas, 2004). These properties are the key issues to understand biochar mechanisms within soil and their potential applications (Sparkes et al., 2011) or carbon dioxide sequestration potential (Downie et al., 2009).

2.2.1. Physical properties

As pyrolysis temperature increases, biochar exhibits greater crystallinity (Keiluweit et al., 2010). Structurally, the bulk structure of biochar is usually non-conductive with pores, complex aromatic-aliphatic organic compounds and minerals (Das et al., 2016), although it has been reported that biochars produced under 500°C exhibits semiconductor properties (Joseph et al., 2013). Biochar is formed mainly by carbon, so the final biochar structure is relative to the highest treatment temperature, having different possibilities.

Firstly, if the aromatic carbon rings were arranged in perfectly stacked and aligned sheets, it needed higher temperatures during pyrolysis (about 500°C). It is possible long-range two-dimensional order of these planes, but not in the third direction. Vanholme et al. (2013) observed that high parameters such as residence time and temperature increase the polyaromatic crystallite cluster and other atoms and functional groups can be located around the edges of these C sheets. The most usual is that which forms highly disordered and irregular structure in amorphous mass, containing other elements than carbon (such as N or O) or minerals depending on feedstock. Those feedstocks (leaves, manures or sewage sludge) rich in phosphorus and nitrogen, permit favour the formation of heteroatomic networks (De la Rosa & Knicker, 2011; Knicker, 2011). Between these C layers, it may be created interstices and voids within hexagonal planes that may be filled with a range of products such as volatiles, tars or other decomposition products.

In some cases the loss structural complexity or porous transformation may occur, following degradation and finally, lost of structure. This fact is associated with plastic deformation, melting, fusion and sintering (Fu et al., 2011) under high temperatures and reaction time or in some kind of feedstock (high mineral ash or very low mineral content), local melting of cell structures, phase transformations and swelling (Jones et al., 2007). At lower heating rates, volatile release occurs readily through the feedstock pores resulting in retention of structural complexity (Cetin et al., 2004).

The surface area is linked to particle size distribution and have strongly influences with its properties including water, air, nutrient cycling and microbial activity. For instance, sandy

soils that have lower surface areas are not able to store water or plants nutrients, whereas clayey soils exhibits large surface areas and high water holding capacities (WHC) (Troeh & Thompson, 2005). It has been suggested that biochar can alter soil physical properties in a similar way. As high temperature and pyrolysis time increase the surface area of the biochar. Nevertheless, pores of different length scales can be formed. Micropores ($<0.2\ \mu\text{m}$) can transport adsorbates within them while macropores ($>10\ \mu\text{m}$) provide a channel for root hairs and may act as habitats for microbes. There is a correlation between micropores volume and total surface area, as pyrolysis temperature increases, surface area increases up still a moment when biochar structure breakdown, causing a decrease in surface area. In addition, it also happens with exposure time; rather, when time grows at the same temperature, there is a point where surface area of biochar decreases (Angin et al., 2013).

The focus issues for surface area of biochar are usually size, density and distribution of micropores rather macropores. Typical densities for biochars are around $1.5\text{--}2.0\ \text{mg m}^{-3}$ (Brewer et al., 2012) due to the amorphous arrangement of the C planes. There are two types of density parameters used to describe biochars. First, *solid density*, which represents the density of the biochar within the solid phases on a molecular level. This density increases with both increasing temperature and residence time because is associated with the conversion of low density disordered C present in feedstocks to turbostratic C (Kercher & Nagle, 2003). It is independent of heating rate, indicating a dependency between density and final process temperature (Brown et al., 2006). On the other hand, *Bulk (or apparent) density* includes solid phases, particle pores and interparticle voids. It is calculated dividing the mass of the biochar sample with its bulk volume, thus an increase in solid density is correlated with a decrease in bulk density.

2.2.2. Chemical properties

Biochar is mainly formed by carbon, generally in form of polycyclic aromatic compounds. The higher the temperature of pyrolysis the more aromatic rings are present, which is accompanied with a decay of biochar yield (Schulze et al., 2016). The carbon content varies enormously depending on the feedstock and pyrolysis conditions. The application of extremely high pyrolysis temperatures reduces the amount of carbon. Beyond a certain threshold, the mass of biochar may decrease without any effect on the carbon amount retained within biochar due to the mass lost goes to the ash content. In addition, biochar contains ashes formed by inorganic constituents (calcium, magnesium and carbonates) (Joseph et al., 2009). The feedstock source and pyrolysis conditions affect to ashes content, determining their potential end uses. For example, biochar produced from wood has the lowest ashes content, meanwhile those from sewage sludge exhibit considerable higher levels (Enders et al., 2012). The pH of biochars ranges from 4 to 12 depending on feedstock and pyrolysis conditions (Lehmann, 2007). Biochars also contain O and N-functional groups (such as alcohols, phenols, carboxylic acids, amines, amides, carbonyls and heterocycles) (Sevilla & Fuertes, 2010).

Cation exchange capacity (CEC) is the ability of the soil to hold cations, so the higher the CEC the more fertile the soil because major mineral nutrient present in the soil are predominantly cations. Low temperatures have generated high CEC biochar while those produced at greater temperatures than 600°C have reduced or not present CEC (Navia &

Crowley, 2010). Fresh biochar exposed to oxygen and water in soil, will suffer an oxidation reaction, as a resulting in a growth in the net negative charge and hence an increase in CEC.

Respecting to nutrient content, biochar reflects nutrient content of the feedstock. Biochar produced from wood generally have low nutrient levels, whereas biochar produced from sewage sludge have higher nutrient contents as well as other micro and macronutrients. High pyrolysis temperatures may decrease nitrogen content and its availability. The remaining nitrogen becomes incorporate into the carbon matrix limiting the availability of nitrogen in the biochar produced (Macías & Arbestain, 2010).

Table 2. Feedstock properties relevant to thermal conversion processes

Feedstock		Wood	Grass	Manures	Sewage sludge			Municipal solid wastes	
					Primary	Activated	Digested	Total	Organic
Elemental analysis	C	50-55	46-51	52-60	53.3	-	54.4	27-55	47-52
	H	5-6	6-7	6-8	7.2	-	7.7	3-9	0.63
	O	39-44	41-46	26-36	32.0	-	29	22- 44	40-42
	N	0.1-0.2	0.4-1.0	3-6	5.3	-	5.6	0.4-1.8	0.16-0.25
	S	0-0.1	<0.02-0.08	0.7-1.2	2.160-80	-	3.2	0.04-0.18	0.002-0.003
Volatile fraction (% db)		70-90	75-83	57-70	25	59-88	30-60	47-71	-
Ash (% db)		0.1-8	1.4-6.7	19-31	25	-	37.5	12-50	0.02-0.2
Moisture content (% fresh weight)		50-20 (dried) 35-60 (green)	NA	21-99.7	90-95	97-99	88	15-40	45-70
Particle size (mm)		NA	NA	NA	<5% (82% wt. <0.1	<5% (66% wt. <0.1	<1 (66% wt. <0.1	0.2-600	0.2-600
Energy content (MJ/kg _{db})			18.3-20.6	13-20	23-29	19-23	9-14	2-14	8.9-11.5

2.3. Evolution of biochar in soil

Once biochar is placed in soil as amendment, their physicochemical and biological propriertes suffer an evolution. The main effects are physical, chemical alteration and persistence.

2.3.1. Physical alteration

With time biochar experiment a physical evolution which include several phenomenon.

2.3.1.1. Fragmentation to smaller particles.

The reduction of the particle size of biochars might follow the same patterns than wildfire-derived particles. The average particle size range on fire-derived products is greater than in biochars (Lynch et al., 2004), which have more uniform composition and size. Fragmentation is determined by the raw characteristics and soil conditions, some studies observed the same fragmentation patterns, regardless the initial wood species in the feedstock (Théry-Parisot et al., 2010). The homogeneity in the fragmentation patterns used to follow a Poisson distribution for all species.

2.3.1.2. Heteroaggregation with other soil particles.

Heteroaggregation is explained by classical Derjaguin-Landau-Verwey-Overbeek (DLVO). That theory describes that the dispersed particles are subject to two types of long-range forces, which influence the fact that two particles are close under the action of Brownian motion, touching reaching and remaining in contact or not (Petosa et al., 2010). Two negatively charged surfaces aggregate via slow, reaction-limited aggregation at low electrolyte concentration due to repulsive electrostatic forces. When electrolyte concentration exceeds the critical coagulation concentration, charge-screening results in fast, diffusion-limited aggregation driven by attractive van der Waals forces (Chen & Elimelech, 2008).

Aggregation is promoted by reactive clays such as smectite and other clays with high CEC, but this is disfavoured by non-expanding, crystalline clays such as kaolinite with low CEC and surface area (Bronick & Lal, 2005). As a result, Al, Fe hydroxides control the aggregation of biochar in acidic soils having low clay and soil OM.

Micropores and non-graphenic structures of amorphous C of biochar are expected to be the active sites where mineral enrichments and other stabilizing interactions occur (Joseph et al., 2010). It can also be affected indirectly by soil conditions, soil mineralogy (clay minerals content, CEC content, etc.) and the biochar itself. Micro aggregation with clay-size particles stabilize low-molecular-weight soil organic matter (SOM) through interaction of SOM with aluminosilicates or amorphous Fe and Al. In addition dissolved cations leads to the formation of microaggregates (size 20-250 μm) (Six et al., 2004).

Heteroaggregation may also protect biochar from chemical and biological reactions, but it has been purposed that biochar rapidly associates with mineral matter and other non-pyrogenic SOM to form aggregates in which the pyrogenic carbon (PyC) (quinone, phenol, ketone and aromatic structures) are occluded within micro confinements. Non-pyrogenic aliphatic C (labile polysaccharides, amino sugars/acids, nucleic acids and phospholipids) are located in nanoconfinements. PyC is protected against further chemical degradation and transport (Brodowski et al., 2006). In fact, very often PyC originating from former vegetation fires represents the oldest organic C form in soil (Pessenda et al., 2001).

2.3.2. Chemical alteration

Chemical alteration refers to changes in oxidation state, O content, pH, point of zero net charge (PZNC), CEC, average fused ring size and preferential loss of C-containing fragments from the biomass body. The understanding of the chemical alteration of biochar in soil is starting to emerge and is still mainly constrained by the analytical methods in use. Proxy methods, such as volatile matter (VM) content, CEC and surface area are operational or

depend on the method chosen. They have limited value for elucidating structures and identifying processes and mechanisms. Also is known that feedstocks and pyrolysis conditions vary the rate of these changes and is hard to know how fast they occur.

Initially some of the C is left with unsaturated valence or “dangling bonds” which can be used to oxygen absorption. Weathering processes alter chemical composition of biochar causing a chemisorption of O₂ in “dangling bonds” and H₂O at the following hours and days to synthesis (Antal & Gronli, 2003). The grade of adsorption of O is influenced by pyrolysis conditions. In addition, alkaline biochar may also react with CO₂ from the air to form carbonates altering surface pH. Oxidance is more pronounced on surfaces than throughout entire biochar particles.

Biochar also content uncarbonized biopolymers and semivolatile pyrolysis oils that together forms the “volatile matter” (VM) content (International Biochar Initiative, 2013). At first year, almost a 10% of VM is readily mineralized in soil, existing a relationship between mineralized fraction and VM. It also has their effects on chemical and physical properties as surface area and pore size distribution. When biochar is heated to mild temperatures (150°C) emits CO₂, hydrocarbon gases and a diversity of volatile organic compounds (VOCs) (Spoukas, 2011). Biochars produced above 350°C tended to emit greater amounts of aromatic compounds and hydrocarbons, which can slowly desorb into the soil, it may affect plant and microbial responses to biochar amendments.

The main effect caused in biochar surface is adsorption of natural organic matter (NOM), biogenic substances (in form of biofilms and microbial exudates) and polysaccharides by classical electrostatic adsorption and diffuse double-layer theories.

Therefore, it is obvious that fragmentation and solubilisation of biochar facilitates its transport in the soil column and may influence its functions in biological processes. However there are many issues that have to be studied respect these aspects, but being compared to wildfire chars, studies indicate that fragmentation is enhanced by weak physical structures in the feedstock (specially decay), increasing temperature and O concentration during pyrolysis and freeze-thaw cycling (Nocentini et al., 2010)

Thank to adsorbent properties of biochar for nutrient retention and stabilization of contaminated soils. Studies have shown that in soil at short term, reduces its adsorptive strength towards organic compounds and changes the shape of the sorption isotherm. Sorption attenuation is mainly due to of the surface by adsorption of non-pyrolytic carbon matter (non-PCM), which competes for sites and shifts the pore size distribution available to other solutes to larger pores. Over long term, surface polarity is changed, and its reversibility is poorly understood (Harvey et al., 2011).

2.3.3. Persistence of biochar in soil

Biochar characteristics and composition generates persistence and therefore longer residence times in soil. This mean that biochar mineralize more slowly than the biomass which they were produced from. The persistence is the property that measure the length of time that biochar remains in soils.

The persistence enhance ecosystem services: the net CO₂ emissions from biomass converted to biochar is reduced which offer opportunities for climate change mitigation

(Whitman et al., 2010); benefits of the presence of biochar in soil continues for longer period of time such as effects of nutrient and water availability or mitigation of agrochemicals or toxins. The enduring presence of the biochar may not always translate into a continuation of any initial positive effects, as its properties can change during exposure of soils (loss of its acid neutralizing ability or polycyclic aromatic hydrocarbons, PAHs absorption).

For estimating the persistence of biochar, several conditions have to meet: (i) the input has to be known or approximated; (ii) physical mass losses other than mineralization have to be quantified (erosion, leaching or burning) ignoring other losses will allow a minimum MRT to be calculated that could lie significantly higher; (iii) more than two points in time have to be available for using differences in PyC stocks.

Charring significantly decreases mineralization of OM by at least one and a half orders of magnitude under identical environmental conditions. The relative decrease in mineralization is significantly related to its OM forms (such as aromatic C) which depends on the way in which the biomass is hydrolysed, mainly by variations in charring temperature and time. This is becoming better predictable though aromaticity, and the atomic ratios of organic C, H and O. Variation between locations, experimental conditions and extrapolation approaches add complexity to interpretation.

2.4. Potential of biochar as sink of carbon in soils

During the pyrolytic transformation of biomass in Py-OM (biochar), a significant part of the OM is condensed in poly-aromatic structures that increases the aromaticity and recalcitrance. The organic matter in soils constitutes approximately 2/3 of the global terrestrial C pool, which corresponds to 4000 Pg to a depth of 3 m (Hernández-Soriano et al., 2013) and therefore, the dynamics of organic carbon (OC) in soils control a large part of the terrestrial C cycle. Carbon dioxide (CO₂) in the atmosphere since the dawn of settled agriculture, about 10,000 years ago. Human activities have caused a net release of CO₂ to the atmosphere of about 800 Gt C per year and particularly, forest conversion to agriculture can release up to 75% of stored soil OC as CO₂. (Batjes et al., 1996). Thus, the application of biochar to soil has been proposed as a valid approach to establish a significant, long-term sink for atmospheric carbon dioxide (CO₂) in terrestrial ecosystems (Sohi et al., 2010). However, these assumptions have to be taken with caution, and the previously common supposition of pyrogenic organic material (PyOM) being inert has long been proven wrong (De la Rosa & Knicker, 2011).

Nevertheless, charring significantly decreases mineralization of OM under environmental conditions, thus biochar mineralize more slowly than the biomass they were produced from. The term soil C sequestration implies transfer of atmospheric CO₂ into soil C pools, preventing the immediate release of CO₂ into the atmosphere from C inputs in soil. This transfer of C helps off-set emissions from fossil fuel combustion and other C-emitting activities while enhancing soil quality and long-term agronomic productivity, reducing net CO₂ emissions from biomass converted to biochar, which offers opportunities for climate change mitigation (Whitman et al., 2010).

Within the context of global climate change biochar has become more and more important since the application of biochar to soil has been proposed as a novel approach

to establish a significant, long-term, sink for atmospheric carbon dioxide in terrestrial ecosystems. Land application of biochar and PyOM is not a new concept. Certain pre-Colombian, archaeological dark earths in the Amazon Basin (so-called Amazonian Dark Earths or "*terra preta*") have received large amounts of charred materials. The on-going, large-scale Terra Preta genesis in Amazonia displays this very slow turnover in soils, indicating that biochar can improve soil fertility besides the climate change mitigation option (Glaser et al., 2012). However, to which extent the longevity applies also to artificially produced pyrogenic material is still not clear and will be examined within the proposed research.

In which concerns C stabilization from PyOM forms, there are a number of detailed studies describing charcoal formation (Knicker, 2007) and associated C dynamics (Preston & Schmidt, 2006), including its role in the global carbon cycle (Schmidt et al., 2000). Biochar is often referred to as a material of high chemical and biochemical stability, which may persist over long periods of time (Kuzyakov et al., 2009). During the pyrolytic transformation of biomass in PyOM (biochar), a significant part of the OM is condensed in poly-aromatic structures, thus the aromaticity and recalcitrance of OM is increased. Nevertheless, that process is also linked to drawbacks and uncertainties. There are evidences that the paradigm of recalcitrant biochar has to be revised, since newer results of our group (Knicker et al., 2013) and of others (Watzinger et al., 2014) indicate that in soils, biochars may be degraded at rates which are only slightly slower than those observed for SOM. Solid-state ^{13}C NMR spectroscopy showed that already after two months of biochemical degradation the chemical structure of grass char was modified (De la Rosa and Knicker, 2011); this degradation includes a partial oxidation of aryl structures.

Biochar contains large amounts of OC. Thus, when applied to land, they have the potential to significantly, increase SOM contents, an aspect that is in critical decline in Mediterranean ecosystems and particularly in metallic, mine spoils. A confident assessment of the stability of the C contained in biochars in a cambisol under Mediterranean climate has not been achieved yet and will constitute one the major goal of this study. One of them concerns the fact that only few is known about the long-term carbon sequestration potential of biochar amended soils in non-tropical zones such as the Mediterranean areas.

3. OBJECTIVES

According to literature, biochar is not well defined because of the variety of factors involved in their characterization. Not all kind of biochars are recommended as soil ameliorants neither for C stabilization. It is strictly required a detailed analysis of all properties of all kind of biochars prior being applied to the soil.

Nowadays, the actual global framework for biochars is focused in three main lines. The first one is the global climate change challenge, caused by the industry emission of greenhouse gases (GHG). The use of biochar in agriculture contributes to the reduction of GHG because it acts as carbon reservoir mitigating the greenhouse effect. On the other hand, due to the world population growth, agriculture and industrial activity leads to an enormous accumulation of residues derived. Production of biochar allows a reduction of waste, biomass and residues generated by these activities. In addition, the application of biochar causes a C-stabilization in soils, more than using the initial feedstocks.

In the recent years, several studies described the short-term effects of biochars on (sub)tropical regions. However, very few is known in which concern the real carbon sequestration potential, stability of biochar and effectiveness at field conditions. Most of essays with biochar are being developed in greenhouses under fully controlled conditions and at a short timescale. To our knowledge, there is no previous studies concerning the effects of aging on the composition, structure and stability of biochars at Mediterranean climate conditions. In addition, the present work it will discuss the efficiency of carbon sequestration under Mediterranean climate conditions of five types of biochar produced from different feedstock.

However, properties turning biochar into a beneficial product for agriculture may be different to that making a biochar useful for establishing a significant and long-term C sink in soils. Therefore, it is necessary to achieve a greater comprehension that would takes into account the relationship between the properties of biochar to agricultural response and its recalcitrance. The major goals of the present Master thesis study are:

1. **Determining the effect of weathering on biochar properties, which were applied to typical mediterranean agricultural soil.**
2. Understanding the relationship between the physico-chemical properties of different biochars and their aging under environmental conditions.
3. Increasing the knowledge of the effects of biochar addition to soils on specific characteristics such as: C and N content, functionality and chemical composition through time, biochemical recalcitrance and assessment of carbon stabilization on biochar amended soils under Mediterranean climate conditions.
4. Discerning the most appropriate biochar to be used for C stabilization in soils under Mediterranean climate conditions.

In order to achieve those goals a multidisciplinary approach has been performed, using different techniques such as elemental (C and N), Field Emission Scanning Electron Microscopy (FESEM) and InfraRed Spectroscopic (FT-IR and ^{13}C - ^{15}N NMR spectroscopy) analyses. Finally, pH, electrical conductivity (EC), fragmentation degree and biochar structure were also determined. The recalcitrance of the biochars has been assessed through a respiration experiment in which the biochars and biochar mixed with soil were

incubated for four months using an automatic respirometer and related to the physicochemical properties of these biochars. This experiment permitted the assessment of the C-sequestration potencial of biochars in a Cambisol, a typical Mediterranean agricultural soil.

4. MATERIALS AND METHODS

4.1 Experimental design of the field experiment with biochar amended soils

The field experiment took place from January of 2014 to March of 2016. It was carry out in the experimental farm “La Hampa” of the Instituto de Recursos Naturales y Agrobiología de Sevilla (IRNAS) which belong to the Consejo Superior de Investigaciones Científicas (CSIC). This experimental research station is located near to Coria del Río (Seville) in the Guadalquivir river valley (SW Spain; 37° 21.32 N, 6° 4.07' W).

The first stage of experiment was performed from January 2013 to August 2013. Seeds of *Helianthus annuus* (sunflowers) were planted using two different doses of biochar as soil ameliorant, 1.5 and 15 t ha⁻¹ respectively. In addition, two plots were settled under similar conditions but no biochar was added, they were used for comparison purposes (control). Five different sorts of biochars were tested. They included material derived from sewage sludge, wood and paper sludge, yielding in 12 different treatments. The soil of the filled experiment is classified as Cambisol (IUSS Working Group WRB, 2007). Seven months after the seeding, sunflower plants were harvested.



Figure 2. View of the area of the experimental area at different stages of the experiment. a) Installation of the experiment during January of 2014 b) Sunflower growing after 2 months C) Monitoring the sunflower growth 6 months after the seeding. D) View of the area at month 24 during the last sampling of biochar.

4.2. Biochar sampling

4.2.1 Description of biochar samples

Five biochar samples were used this experiment. These biochars employed in this work were produced from different feedstock: pine wood (PWB), paper-sludge (PSB), sewage sludge (SSB), kiln-wood biochar (KWB) and mixed wood chips (or certified biochar) (CWB). Production conditions for each biochar are showed in Table 3. Four of them (PWB, PSB, SSB and CWB) were provided by the European Rig Trial, organized by the Biochar COST titled “Biochar as option for sustainable resource management” (action TD1107). The Biochar Ring Trial is a blind essay where information about the feedstocks, production conditions or the pyrolysis equipment used are known only by several members of the COST Action committee. The kiln wood biochar (KWB) was provided by the Spanish winery Torres (Bodegas Torres S.L.), it was produced in kilns, a traditional carbonization methodology.

Table 3. Production details of biochar samples

Details	PWB	PSB	SSB	KWB	CWB
Producer & location	Swiss biochar, Laussane, Switzerland	Sonnenerde GmbH, Austria	Pyreg, Germany	Bodegas Torres, Spain	Swiss biochar, Laussane, Switzerland
Feedstock	Mixed wood sieving from pine wood chip	Paper sludge & wheat husks	Sewage sludge (DM 75%)	Vineyard wood (>1 year old)	Mixed wood chips, biochar Europe certificate
Duration of pyrolysis	20 min	20 min	20 min	>60 min	Unknown
Temperature	20-620 °C	20-500 °C	20-600 °C	Unknown	450-600 °C
Inert gas	None	None	None	None	None
Quenching	With water to 30% water content	With water to 30% water content	With water to 30% water content	None	Unknown

After the pyrolysis, biochar samples were homogenized and dried at 40°C during 72 hours for eliminating moisture. Due to the big size and heterogeneity of biochar KWB, it was grounded to reduce size range of the fragments obtained and sieved (<1 cm). Once the homogenization of biochars was completed, they were stored in plastic bags and refrigerated at 4 °C until use. Low temperatures are required in order to avoid physicochemical alteration of biochar because of microbial degradation (Lehmann et al., 2010).

4.2.2. Sampling procedure

In order to assess the effects of aging on the composition and C stability and persistence of biochars under environmental conditions, biochar samples were hand-picked from the

soils at the plots located at “La Hampa” experimental station at 6, 12 and 24 months after the soil amendment.

The soil sampling was carried out after the removal of the plant cover formed on the upper soil horizon with a pick and a hoe (Figure 3a). Then a drill was used to extract 30 cm of soil profile. Five replicates were taken and combined for each biochar. Samples were transported in glass bottles to the laboratory. Once there, the soil block was dried at 40°C during 72 h and subsequently small branches, fresh mosses, plant remains, roots and soil fauna were removed manually.

Finally, the biochar fragments were carefully hand-picked to separate biochar material from the soil matrix (Figure 3b). Finally, biochar a part was conserved for FESEM was grounded using an agate mortar but another part was conserved for FESEM, placed in plastic containers and stored at 4 °C until their use, following the same treatment and conservation than the original biochar samples.



Figure 3. A) Soil sampling at field experiment 24 months after seedling. B) Carefully hand-picked procedure for the separation of biochar fragments from de matrix

4.3. Methodology

The five types of original biochar as well as samples collected from the field experiment at 6, 12 and 24 months underwent a series of tests. Among which a physicochemical analysis first noted when the pH is measured, the electrical conductivity (EC), water holding capacity and ash content. Then samples are characterized by spectroscopic analysis, including chemistry biochars at different times and physical characterization by ^{13}C Solid-State Nuclear Magnetic Resonance Spectroscopy and Fourier Transform Infrared Spectroscopy (FT-IR) and Field Emission Scanning Electronic Microscopy (FESEM). Finally, a respirometry (Respicond) in which the activity of soil microorganisms is measured is performed.

4.3.1. Physicochemical analysis

4.3.1.1. Micro-elemental analysis (C, N)

For bulk soil and all biochars at every time total carbon (TC) and nitrogen (N) concentrations were determined in triplicate by dry combustion (1000°C) using a LECO Truspec micro CHNS (LECO, United States) for analysis of biochar located in the Centro de Investigación Tecnológica de la Universidad de Sevilla (CITUS). The samples proceeding

from respirometer experiment were analysed by Flash 2000 Combustion Elemental Microanalyzer (Thermo, Germany). Samples were grounded to 1 mm and dried (105°C) during 6 hours before analysis. This equipment measure the amount of these elements by dry combustion method (975°C) detecting N as N₂, C as CO₂ and H as H₂O. The coefficient of variation between replicated analyses was below 5%. Soil samples were subjected to decarbonatation (2 M HCl) prior analysis of the total organic carbon (TOC) content.

4.3.1.2. pH and Electrical conductivity

Aliquots of each type of biochar samples were taken, mixing biochar with distilled water in a ratio of 1:10 (biochar: H₂O). The mixture was stirred for 30 minutes to achieve a homogeneous suspension. The suspension was measured in triplicate for each sample with a pH/EC meter Crisom 40 pHmeter and Crisom Basic 20 conductimeter (Crison, Spain).

4.3.1.3. Biochar fragmentation

The fragmentation of biochar particles during the field experiment was determined by accounting the the number of biochar fragments of the starting biochar samples and of the hand picked biochars, which were kept at field during 6, 12 and 24 months. The method consisted on weighting 200 mg of each type of biochar randomly and the total number of fragments was count three times for each sample. This methodology considers that the greater the number of fragments an enhanced fragmentation of biochars is occurring (Pereira et al., 2014).

4.3.2. Fourier Transform Infrared Spectroscopy (FT-IR)

4.3.2.1. Theoretical fundaments for application of FT-IR spectroscopy in soils

Fourier transform infrared spectroscopy has been used extensively to understand the development and alterations in functional group chemistry of biochars. This technique is based in the different frequency of vibration of the atoms of molecules that allows knowing what their molecular structures of the samples are. The absorption happens when the frequency of the IR radiation is the same than the vibrational frequency of a determined bond. The derived frequency of the emission when it is detected cause the apparition of bands in the respective infrared spectrum. The results are given in transmittance or absorbance using a Fourier Transform instrument, which can be attributable to a specific group of chemicals.

The theory is based on the fact that the atoms can vary the distance between them or even also move out of its present plane. These phenomenon are described as stretching and bending movements (vibrations). Therefore, for a diatomic molecule, only possible one vibration corresponds to the stretching and compression of the molecule (one degree of vibrational freedom). In the case of polyatomic molecules containing n atoms, it will have 3n degrees of freedom (Plischke & Bergersen, 2005). The factors that depend on the value of frequencies are mass weight (μ) and strength constant (κ). Generally, the lighter molecules the higher frequencies are associated to them, so when heavier are the molecules bonded lower frequencies they have. For the case of C atom when the mass is reduced, μ , increases, the frequency decreases. In the case of strength constant (κ), the higher strength constant the higher frequency, so it depends of the type of bond (simple,

double or triple). For example, the strength constant for the C=C bond is approximately about twice than C-C.

Treating the IR spectra of samples biochar it is an arduous task due to the multiple functional groups, which may be responsible of the multiple bands in their respective spectra. Another drawback might biochar samples from sewage sludge have a high mineral content, which can originate bands that overlap with the oxygen functional groups of the sample (Zielinska, 2015).

4.3.2.2 Applied conditions for FT-IR spectroscopy

Fourier transform infrared spectra were performed using Bruker Tensor 37 FT-IR spectrometer from 4000 to 800 cm^{-1} , using a resolution of 2 cm^{-1} . Potassium bromide pellets were prepared using 1-0,5% (w/w) of each biochar. It consisted on transferring into a agate mortar 1 mg of biochar, which was finely grounded and mixed with 100 mg of potassium bromide (KBr) previously dehydrated and grounded to a fine powder. Then the content of the mortar were placed in a cylindrical piston under high pressure and vacuum. A total of 60 scans were accumulate for each spectrum in order to improve it and get a higher resolution All IR data treatment was carry out using OPUS spectra manager software®. The samples analysed by this technique were all the biochar samples (original and aged at different times) and the samples taken from respicond respirometry analysis.

4.3.3 ^{13}C Solid-State Nuclear Magnetic Resonance Spectroscopy

4.3.3.1. Theoretical fundaments for application of NMR spectroscopy in soils

The Nuclear Magnetic Resonance (NMR) is the most useful spectroscopy technique to obtain structural information. This technique is based on the absorption of radiofrequency radiation by atomic nuclei and the influence of their neighbour atoms in presence of an external magnetic field of solid and aqueous samples. NMR provide different information depending on the sample and technique used for acquisition of spectrum such as structure, dynamics, reaction state or bulk functional group classification (Lorenz et al., 2004).

In soils, the most usual types of NMR used is ^{13}C - and ^1H NMR. Their combination permit a successful determination of organic compounds without a pre-treatment of the soils. Thought this technique is given the determination of gross chemical composition of the material under study, quantitatively correlation between the signal intensities and contribution of the respective C and H types to the total C and H content. The combination of both types of MNR deduce the structure of carbonate skeleton over the surrounded effect of ^{13}C and ^1H with the Cross Polarization Magic Angle Spinning (CPMAS) technique (Wilson, 1987). The magnetization of a sensitive spin as ^1H with another element of lower natural abundance as ^{13}C , obtain an improvement in NMR spectral resolution, phenomena called Hartmann Hahn contact. After transfer, the frequency of magnetization of the least abundant element is detected. Specifically, the NMR used is based on applying to the sample a turn at high speed long around the magic angle to get a narrow 54.74° in order to average line broadening induced by the low molecular motion in solids (Knicker al., 2005; Lian & Roberts, 2011).

Table 4. Chemical shift assignment of various peaks in a ^{13}C NMR (Knicker et al., 2007). For samples shift assignment did not necessary adjusted to the same range.

Shift (ppm)		Assignment	
10-45		Alkyl-C	
45-90		O- and N-alkyl	
	45-60		Aliphatic C-N, methoxyl
	60-90		Alkyl-O (carbonates, alcohols)
90-160		Sp ² -hybridized C	
	90-140		Aryl-H and Aryl-C carbons, olefinic-C
	140-160		Aryl-O and aryl-N carbons
160-210		Carbonylic-C, carboxylic-C, amide-C	
	160-185		Carboxyl and amide-C
	185-210		Aldehyde and ketone C

4.3.3.2. Applied conditions for ^{13}C NMR experiments of biochar samples

Cross-polarization magic angle spinning (CPMAS) ^{13}C NMR experiments were carried out on a Bruker Ascend 400 MHz (Bremen, Germany). The samples of biochar were grained and homogenized being placed into zirconium rotors of 4 mm OD with KEL-F-caps. The rotors were spun at 14 kHz. A ramped ^1H -pulse was used during a contact time of 1 ms in order to avoid a loss of signal due to the circumvent loss of selective signal intensity due to the spin modulation (Hartmann-Hahn contact). A 90° ^1H -pulse width of 2.4 μs is used for all spectra. The ^{13}C -chemical shifts were calibrated relative to tetramethisilane (0 ppm) with glycine (176.04 ppm). Over 10,000 scans were accumulated for each sample; having a pulse delay between the single scans of 300 ms.

For solid-state ^{13}C NMR samples biochar there is a characteristic for each of the frequency shift. In Table 4 the relative intensities of each, which were obtained by routine integration with software NOVA MESTRE. The ^{13}C NMR spectrum of PWB could not be acquired because of the impossibility to tune the probe containing the sample before to the measurement. The explanation to this fact could be explained by the graphitic content of this biochar sample. The result is that this graphitic compounds lead to a heating up of the electrons that could cause major damage to the NMR equipment.

4.3.4. C stabilization in biochar by using a respiration experiment (Respicond)

4.3.4.1 Theoretical fundamentals of Respirometer Respicond®

The respirometer system is a device with a fully systematic sampling system, so that allows acquiring data every hour for several months. The device consists in 96 jars immersed in a water bath. Each of these jars contains within the electrodes, which are connected to a conductimeter, immersed in the KOH solution. In the Figure 5 is shown the basic unit.



Figure 4. Image of Respicond Apparatus IV (Nordgren Innovations, Sweden)

Data provided by this device by biochar or biochar-soil incubation samples offers important information about the variables which affect microbial activity as substrate decomposition. Microbial respiration has also been used as a means of determining microbial biomass (Jenkinson & Powlson, 1976) and of estimating maintenance requirements of fungi and bacteria (Anderson & Domsch, 1985). This system has the purpose to measure the CO₂ release of samples after absorption in a KOH solution giving as product CO₂⁻³ ions as a decrease of the electrical conductivity of solution. The production of CO₂ or the loss of C can be plotted respect time. Total C contents and mass weight were measured at the beginning and the end of the incubation. For fit was used Sigmaplot II (Sustyt software Inc.) according to Eq. (1):

$$A(t) = A_1 \times e^{-k_1 t} + A_2 \times e^{-k_2 t} \quad (1)$$

Where: A (t) is the remaining C (% of total C_{org}); A₁ is the amount of C which is relatively labile against mineralization (% of total C_{org}); A₂ is the amount of C which is more stable against degradation (% of total C_{org}); t is incubation time; k₁ and k₂ are apparent first order generalization rate constants for the labile and refractory pool (y⁻¹). Consequently, the mean residence times of the first order reactions are equal to 1/k₁ and 1/k₂, whereas the half time of A₂ was determined by $t^{1/2} = 0,693 / k_2$. Which slow and fast decay fractions, equivalent to k_s and k_f constants respectively, their mean residence times (MRT_f = 1/K_f and MRT_s = 1/K_s) and their halftime times (t_{1/2}) = MRT ln 2 (Nordgren, 1988).

3.4.2 Conditions of the experiment

Biochar samples were incubated at 60% of the WHC after inoculation with a microbial suspension. For each vessel, it was taken samples of the homogenised field, containing the mixture of cambisol and biochar with each type of biochar. In each of the vessels was inoculated 1 mL of a microbial suspension obtained from the fraction of soil on the field trial prefiltered distilled water (Whatman 2) was performed.

Each vessel (Figure 5) was incubated for 108 days (from 27th of January to 10th of May of 2015) at mean temperature of 26°C under aerobic conditions in a Respicond Apparatus IV (Nordgren Innovations, Sweden). The CO₂-released was monitored every 2-3 hours for a period of six months. The respiration was measured every 3 hours by determining changes in the electrical conductivity induced in the absorption of CO₂ in 10 mL of a 0.6 M KOH solution placed inside the vessel and the mix (Nordgren, 1988).

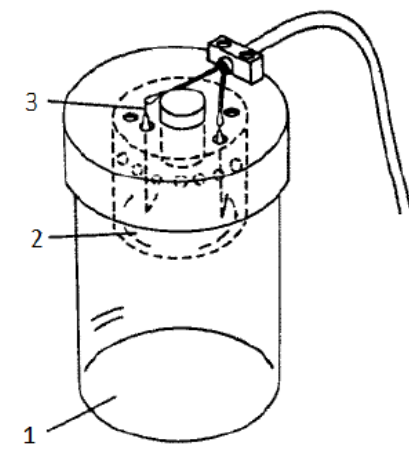


Figure 5. Representation of the jar used in Respicond. 1) Vessel where the sample is placed; 2) Cell where is placed the KOH dissolution; 3) Electrodes. (Nordgren, 1988).

Through multiple techniques to study biochar chemistry can significantly improve characterization and comparisons between samples at different stages since its application. It is used this strategy in the study to complement both techniques each other due to examine the variation of chemical composition of ¹³C and functional groups.

4.3.5. Field Emission Scanning Electron Microscopy (FESEM)

4.3.5.1. Applied conditions for FESEM

Field emission scanning electron microscopy (FESEM) was used to obtain an accurate assessment on surface topography and chemical microanalysis of biochar samples after 2 years of aging under field conditions. Bulk fragments were directly mounted on a sample stub and sputter coated with gold/palladium film. Subsequently, samples were examined on a Jeol JSM-7001F microscope equipped with an Oxford X-ray energy dispersive spectroscopy (EDS) detector using standard ZAF corrections that allow semi-quantitative microanalysis. FESEM examinations were operated in secondary electron (SE) detection mode with an acceleration potential of 15 kV.

5. RESULTS AND DISCUSSION

5.1. Analytical characterization of biochars and soil

5.1.1 Macro-elemental composition of original biochars

Macro-elemental composition (C and N) and selected physical and chemical properties of the five biochars sampled at 0, 6, 12 and 24 months, and the cambisol are given in Table 5. Concerning the soil, pH (in H₂O) was 8.6 and the conductivity was 68 $\mu\text{S cm}^{-2}$. It contained 20 g kg⁻¹ of C (6 g kg⁻¹ Total Organic Carbon, TOC) and 1 g Kg⁻¹ of N.

Respecting to macro-elemental composition, biochars PSB, KWB and CWB, produced from wood, they showed comparable C contents (about an 800 g Kg⁻¹). The PSB sample, which was produced from paper-sludge, contained around 500 g kg⁻¹ of C, whereas SSB (from sewage-sludge) had the lowest C content (less than 200 g Kg⁻¹). It is clear that the nature of the feedstocks affects the carbon content of biochar product (Zhao et al., 2013). Taking into account that KWB and PWB were produced from wood by using different pyrolysis process, we can say that in our case that the main factor for C content is the feedstock and not the pyrolysis process, which is in agreement with Sohi et al. (2010) and Zhao et al. (2013).

Table 5. C and N content of fresh biochars obtained and those levels consulted in the bibliography. Extracted from Bellantini et al., 2012; Brewer et al., 2012; Borchard et al., 2012a; Enders and Lehman, 2012a; Hale et al., 2012; Rajkovich et al., 2012; Oh et al., 2012.

Biochar	Feedstock	Study level		Bibliography	
		C (g Kg ⁻¹)	N (g Kg ⁻¹)	C (g Kg ⁻¹)	N (g Kg ⁻¹)
PWB	Pine wood	847.7 \pm 2.0	1.9 \pm 0.2	>850-746	0.8-0.7
PSB	Paper sludge	475.4 \pm 4.3	12.3 \pm 0.1	238-190	1-2
SSB	Sewage sludge	182.0 \pm 2.1	20.0 \pm 0.4	238-150	1-2
KWB	Kiln-wood grapevine	752.6 \pm 13.4	1.7 \pm 0.0	>800-700	1-2
CWB	Certified wood	829.4 \pm 2.3	0.9 \pm 0.0	>800-746	0.8-0.7

Table 5 shows a comparison between the amounts of C and N obtained for each type of biochar and their values of C and N content according to the bibliography. The amounts of C content of the biochars used for this study are in agreement with those obtained by previous studies for similar biochars (De la Rosa et al., 2014). Most of the biochars produced by enriched-wood raw materials (such as plant-base feedstocks) contain above 500 g kg⁻¹ of C because this material has a high lignin or form heat-resistant compounds content (as furans) (Brewer et al., 2012), which can not be degraded during the pyrolysis process. On the other hand, respecting to SSB sample initially contains considerable amounts of peptidous materials which are less resistant to heating than lignin or furans and easier to degrade at higher temperatures (Knicker et al., 2010). In addition, this biochar is usually very rich in minerals due to the presence of ashes which explains the low carbon content of the sample.

Concerning the nitrogen (N) content (Table 5), PWB, KWB and CWB resulted in lower N contents than SSB and KWB, being the highest amounts of N for SSB (2 g kg⁻¹). Previous

studies showed the contributions of N in biochars. Usually wood biochars containing 1-2 g kg⁻¹ (Enders et al., 2012). For SSB and PSB the N content has huge differences of an order of magnitude than others derived from similar feedstocks as it ensues with C. Aside from the C/N ratio of the source material, the N content of biochars also depends on production conditions (Wu et al., 2012).

5.1.2. Macro-elemental composition of aged biochars

In Figures 7 and Figure 8 it had been represented C content and N content (g Kg⁻¹) in each time to evaluate the C through time. For each graph, the C and N content in the picture because it may be committed a probable error during measurement for both elements.

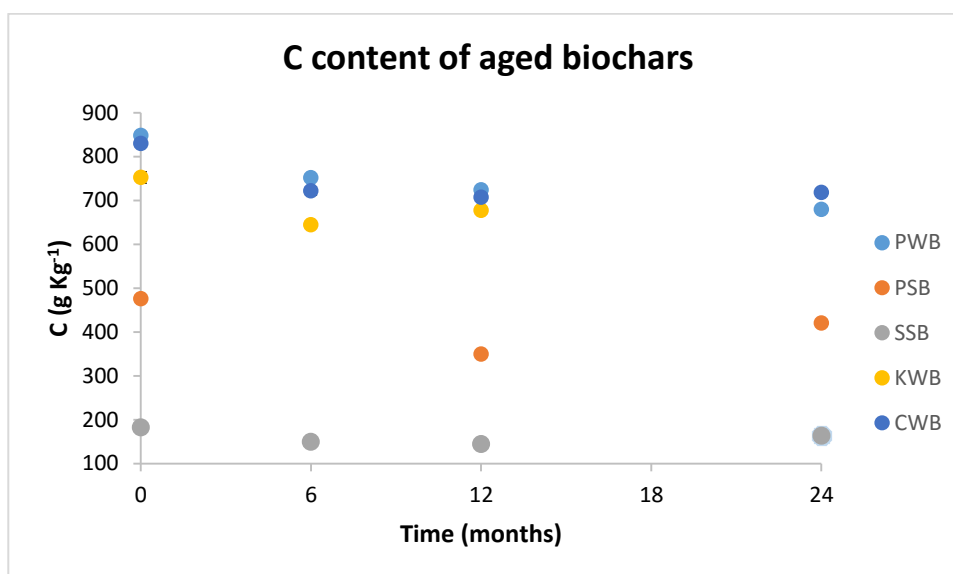


Figure 7. Graphic representation of loss of C at 0, 6, 12 and 24 months. Deviations are in some cases smaller than the labels, thus they are not shown.

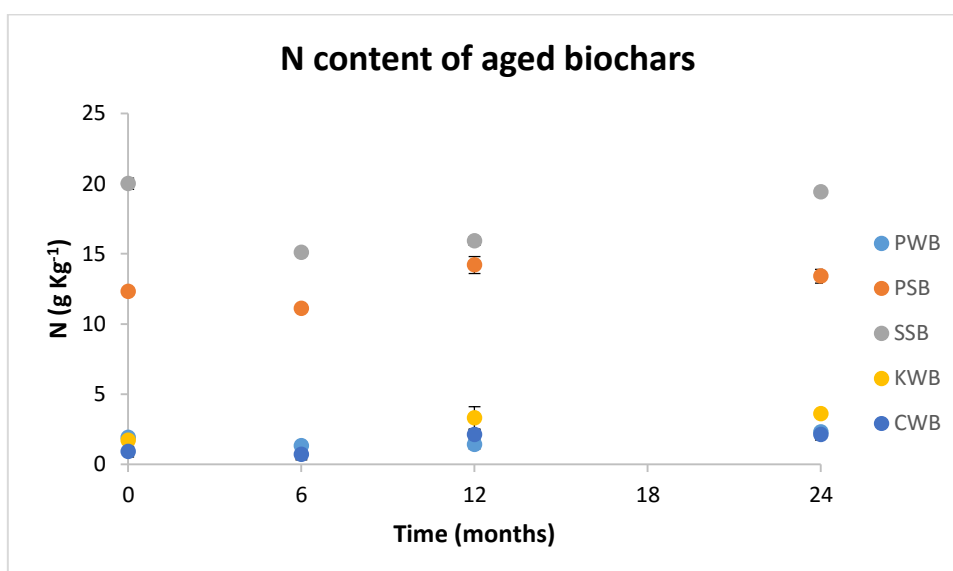


Figure 8. Graphic representation of loss of N at 0, 6, 12 and 24 months. The deviations are in some cases smaller than the labels, thus they are not shown.

An interesting aspect of this research would be based on the study of carbon and nitrogen variation experienced by different types of biochars with time of exposure to field conditions. Initially, during the first six months, there was a strong variation of carbon for all biochars, more pronounced for sample PSB. PWB, CWB and KWB also suffer a reduction in C content, while biochar SSB showed a different behaviour than the rest losing lower amounts of C, at short and long-term, probably for its low content of carbon. For longer periods of exposure the C content experimented a light rise or maintain their carbon content still 24 months, maintaining values of C lower than the original samples of biochar but close to their original.

Respecting to N content, due to their low content (<0.2%) it is difficult to establish a general tendency (Figure 8). Samples PSB and SSB (which had the highest levels o N) reduced their N content after 6 months. The rest of samples (PWB, KWB and CWB) showed no significant alterations of their N content. However, after 12 months there was a light growth in the relative N abundance due to the aggregation of SOM and soil particles to biochar pores (De la Rosa et al., 2014). This reduction is caused when water penetrates into the pores of the biochars, dissolved salts and ions contained therein. So that these ions are dragged to the ground or being dragged deeper soil layers, which decrease the conductivity of the samples (Wu et al., 2014).

5.2 Physical characterization

5.2.1. Fragmentation

Table 6 shows the number of biochar fragments per 200 mg of sample.

Table 6. Number of particles obtained weighting 200 mg of biochar at different time (6, 12 and 24 months).

Sample	No. of fragments per 200 mg (6 months)	No. of fragments per 200 mg (12 months)	No. of fragments per 200 mg (24 months)
PWB	16.3 ± 1.8	13.3 ± 0.4	25.3 ± 2.1
PSB	9.8 ± 1.1	18.0 ± 1.4	28.0 ± 2.80
SSB	17.0 ± 1.4	15.8 ± 1.1	20.3 ± 1.1
KWB	3.3 ± 0.4	3.8 ± 0.4	7.8 ± 0.4
CWB	5.5 ± 1.4	8.8 ± 0.4	16.0 ± 2.1

The number of biochar fragments are increasing with time at field expousure for all biochars. It is also noted that the degree of fragmentation is not homogenous depending on the type of biochar. Of the five types used in the field test, the KWB showed less fragmentation, while the PWB and PSB presented the opposite trend. The maximum fragmentation was achieved after 24 months. Thus, the greater the exposure time, the greater the fragmentation and therefore biochar decomposition.

The fragmentation of the studied samples followed the order PSB> PCB> SSB> CWB> KWB. Nocentini et al. (2010) proved that among the variety of factors responsible for the physical fragmentation of biochar, fragmentation would be directly related to initial structures from feedstock. However, the role of the raw material in its subsequent

fragmentation in soil is not well-defined to date. In our case, the biochars produced from paper sludge and pinewood resulted in the greatest fragmentation degrees. Belcher et al. (1968) confirmed that fragmentation increases with increasing temperature and O concentration in the atmosphere during pyrolysis. This hypothesis indicates that KWB was probably produced at a lower temperature or lower O concentration during the pyrolysis than the other biochars (Table 3).

5.2.2. pH and electrical conductivity (EC)

As it can be observed in Table 7, pH of initial biochars (t_0) PWB, PSB, KWB and CWB, were alkaline ($\text{pH} > 9$), while biochar SSB was neutral (around 7). According to De la Rosa et al (2014), this difference is caused by the nature of the feedstock. Sludge biochars use to have lower pH than plant biomass derived biochars (Agrafioti et al, 2013). In the case of plant derived biochars (the alkaline ones), pH values were reduced with time, reaching values for all the aged biochars within the range 7.7 to 8. The pH of SSB sample increased from 6.9 (t_0) to 7.7 (t_3). Consequently, pH of aged biochars achieved similar values, very close to that measured for the alkaline cambisol. Considering that pH values tend to increase with production temperature (Wu et al., 2014), these data are in accordance with the previous data in which SSB was produced at a lower temperature than the others biochars.

Respecting to electrical conductivity (EC), all biochars showed EC values up to $1000 \mu\text{S cm}^{-1}$, excepting for biochar SSB that has a lower conductivity (about $800 \mu\text{S cm}^{-1}$). Electrical conductivity is responsible for exchange of ions, being their values similar to those obtained by Lehmann (2007) and Liu & Zhang (2012) demonstrating that the properties of biochar were, as pH, dependant on the production procedure and type of feedstock. The EC is often used to estimate the amount of ions thus mineral nutrients in soils. The low value obtained for SSB indicates a low contribution of salts, which is in agreement with its low pH. The evolution through time showed a sharp decline in the EC of biochars, which finally achieved very low values compared with the original biochars ranging 74.5-150.4 $\mu\text{S cm}^{-1}$. It can be explained by the leaching of salts and ions that biochars content within (Wu et al., 2014).

5.3. Elemental composition of biochars

One of the most common analytical approaches to assess the structure of biochar are the use of the elemental ratios H/C and O/C, which is supported by the “*van Krevelen*” diagrams, that define a space determined by a X axis of atomic O/C ratio and a Y axis of atomic H/C ratio. Numerous compilations of elemental ratios of biochars under variety of conditions are available, such as Schimmelpfennig & Glaser (2012).

Once introduced into the soil, the first modification in the structure of biochar is functionalization of the surface with O-containing functional groups. For instance, Joseph et al. (2010) retrieved biochar after two years in soil and O/C ratio of soil age biochar had increased from 0.2 to 0.75. This is caused by a loss in aromatic type C and a growth in O containing functionality from absorption of OM and/or oxidation of the biochar surface. N containing is also increased caused by the contained functionality of proteins, peptides, ammonium and C-N groups. In Figure 9, there are showed the position in *van Krevelen diagram* of the initial biochars used in the present study.

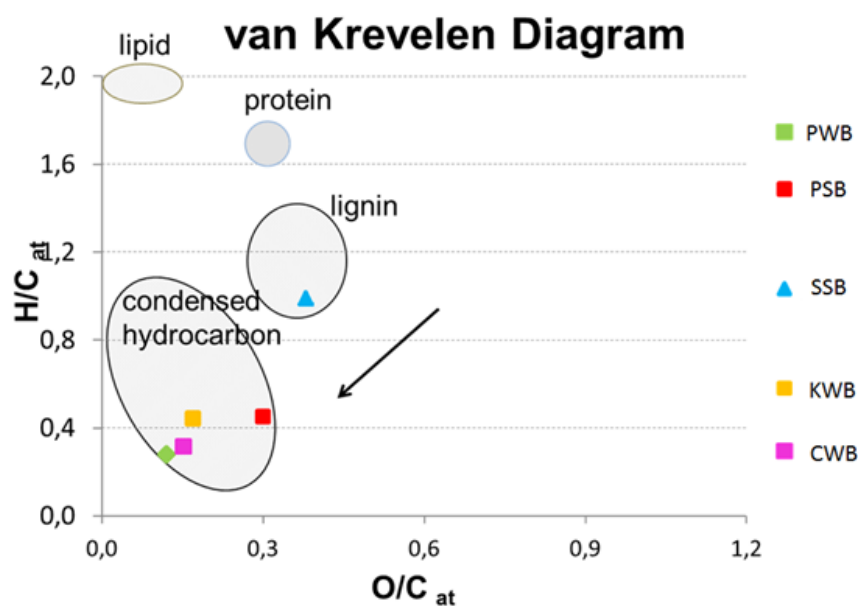


Figure 9. van Krevelen diagram of the five biochar samples (PWB, PSB, SSB, KWB & CWB)

In Figure 9 is shown the five types of biochar, four of them (PWB, PSB, KWB, CWB), have similar H/C_{at} and O/C_{at} values, but respecting to biochar SSB, so it is expected that its properties varies respect the other four. This is due to its high values of oxygen and hydrogen, creating higher ratios of H/C and O/C . The order from higher to lower values of O/C_{at} is: $SSB > PSB > KWB > CWB > PWB$. Respecting the H/C_{at} ratio the order of samples is: $SSB > PSB > KWB > CWB > PWB$, being identical the order for both kind of ratios.

An important agronomical factor would be the relationship between C/N , since proportion essential information on the availability of soil nitrogen. Due to the high carbon content of most samples biochar, a high content of the same, in relation to the carbon makes it difficult for plants bioavailable of a sufficient amount of nitrogen by high amounts of carbon. For this reason the C/N ratio is used, typical values for soils is, so you can would find suitable from 7 to 30 C/N ratio.

Of all initial biochar studied it is shown in Table 7 that the biochar that provided the best C/N ratio is SSB ($C/N = 9.1$) at initial time, followed by PSB ($C/N = 38.7$). These values are preferable than those got by the soil which is below the recommendable C/N ratio ($C/N = 2$). For the rest biochar, it is easy to know that the high C content makes less available the N in soils. Along time for all biochars the evolution of C/N ratio is that all experimented a decrease, due to the C reduction as it was mentioned before. The C/N ratios of SSB and PSB were practically unaltered after 2 years at field, which is a good indicator from an agronomical point of view. Nevertheless, the rest of biochars reduced their ratio, (they showed C/N above 150).

Table 7. Macroelemental analysis and physicochemical properties of the biochars in a field experiment at different times applied to a Cambisol soil used for the incubation experiment. In which t_0 = fresh initial biochar; t_1 = 6 months; t_2 = 12 months; t_3 = 24 months.

Sample	Feedstock	Elemental analysis (C. N)			Physicochemical properties	
		C (g Kg ⁻¹)	N (g Kg ⁻¹)	C/N	pH	Electrical Conductivity (μS cm ⁻¹)
PWB (t_0)	Wood	847.7 ± 2.0	1.9 ± 0.2	446.2	9.3 ± 0.1	1187.7 ± 56.6
PWB (t_1)		751.3 ± 9.2	1.3 ± 0.1	557.9	8.7 ± 0.2	1181.5 ± 50.1
PWB (t_2)		723.7 ± 3.4	1.4 ± 0.7	516.4	7.9 ± 0.1	1179.7 ± 57.7
PWB (t_3)		679.4 ± 1.6	2.3 ± 0.3	295.4	7.9 ± 0.1	101.3 ± 4.2
PSB (t_0)	Paper sludge	475.4 ± 4.3	12.3 ± 0.1	38.7	9.2 ± 0.1	1045.7 ± 13.7
PSB (t_1)		N/A	N/A	N/A	8.6 ± 0.0	989 ± 25.5
PSB (t_2)		349.1 ± 2.8	14.2 ± 0.6	24.6	7.8 ± 0.1	190.5 ± 5.1
PSB (t_3)		419.8 ± 10.5	13.4 ± 0.5	31.3	8.0 ± 0.0	139.5 ± 1.7
SSB (t_0)	Sewage sludge	182.0 ± 2.1	20.0 ± 0.4	9.1	6.9 ± 0.1	814.0 ± 34.4
SSB (t_1)		149.0 ± 1.1	15.1 ± 0.1	9.9	7.1 ± 0.0	801.2 ± 12.9
SSB (t_2)		144.4 ± 3.1	15.9 ± 0.3	9.1	7.7 ± 0.1	117.3 ± 0.3
SSB (t_3)		163.3 ± 1.4	19.4 ± 0.3	8.4	7.7 ± 0.1	150.4 ± 2.5
KWB (t_0)	Kiln wood grapevine	764 ± 10.4	6.0 ± 0.0	127.3	9.3 ± 0.0	1082.3 ± 2.9
KWB (t_1)		752.6 ± 13.4	1.7 ± 0.0	442.7	8.9 ± 0.1	1079.9 ± 25.8
KWB (t_2)		644.2 ± 5.5	3.3 ± 0.1	117.1	8.1 ± 0.1	112.0 ± 1.3
KWB (t_3)		676.8 ± 4.1	3.6 ± 0.1	188.0	7.8 ± 0.0	74.5 ± 0.9
CWB (t_0)	Certified wood	829.4 ± 2.3	0.9 ± 0.0	921.6	9.3 ± 0.0	1096.7 ± 5.1
CWB (t_1)		721.6 ± 9.3	0.0 ± 0.1	721.6	8.7 ± 0.1	1070.1 ± 8.5
CWB (t_2)		707.0 ± 0.9	2.1 ± 0.3	336.7	8.1 ± 0.1	222.7 ± 3.8
CWB (t_3)		718.0 ± 4.1	2.1 ± 0.3	341.9	7.8 ± 0.1	93.3 ± 4.4

5.4. Fourier transform infrared spectroscopy (FT-IR)

5.4.1. FT-IR spectroscopy of initial biochars

Figure 10 represents the FT-IR spectra for the five biochars at initial time (t_0) and after 24 months (t_2) of being incorporated to soil to Mediterranean climate conditions. In general, for all biochar samples except SSB are composed by similar functional groups. Whereas for some of them, differences were detected, especially for SSB.

Firstly, it will be compared the differences between biochars at initial time (t_0). The first peaks appearing in the spectra around $3600\text{--}3350\text{ cm}^{-1}$ in all samples are assigned to -OH vibrations (Hossain et al., 2011). In addition, the bands centred about 3400 cm^{-1} for some of the biochar samples are assigned to some inorganic compounds, in our case, to carbonate compounds (Socrates, 2001). The broad signals around $3000\text{--}3100\text{ cm}^{-1}$ that are attributed to aromatic C-H groups, rather, the aromatic compounds existing in all biochar samples. These bands have observed a loss of the signal intensity corresponding to O-H and aliphatic C-H stretching because of the rehydration of cellulosic and ligneous components due to heating of the samples PWB, KWB and CWB (Zaho et al., 2013). Due to the original feedstock, the sample SSB did not show these kind of peaks whose feedstock was sewage sludge containing a low content rich in cellulose and ligneous compounds are very low.

All spectra (excepting for biochar SSB) shows a peak about 1700 cm^{-1} , which is assigned to aromatic C=C bending and alquene C=C stretching. The fact that these kind of signals does not appear those for SSB, being according to the lower contribution of the aromatic C than the rest of the other four biochars. It could be confirmed using solid-state ^{13}C NMR spectroscopy. This band could be assigned to -COO anti-symmetric stretching of amino acids (Zaho et al., 2013). The signal of this band is bigger for aged biochars as it will be proved for all samples. Close to this peak appear a kind of shoulder near to 1700 cm^{-1} .

Respecting to the FT-IR spectrum of PWB biochar exhibits a peak in 1500 cm^{-1} , originated from graphide molecules (Francioso et al., 2011). This phenomenon is only shown by sample PWB, probably due to its a high condensation degree as it was reported for similar samples by De la Rosa et al. (2014). This kind of spectra has been observed in the IR spectra of other sewage sludge biochars (Hossain et al., 2011), and even it can be caused due to N-H vibration or to O-H stretching caused by moisture. Considering the high nitrogen content, this band should probably to the presence of these nitrogen-rich compounds between all possibilities mentioned before.

Other important peaks were those existing in biochar in PSB and CWB have a common peak at $1586\text{--}1531\text{ cm}^{-1}$ caused by the aromatic C=C vibrations, formed by heat induced dehydration of cellulose, and to aromatic C=O vibrations (Wu et al., 2012). This signal would decrease rising temperature and was observed for some feedstocks studied by Zaho et al. (2013). The signals at the range $1473\text{--}1409\text{ cm}^{-1}$ are typically assigned to aromatic C=C vibrations. This signal can exhibits great variations in the wavelength when it is been comparing different feedstocks but remained almost unaltered when changing the production temperature (Zhao et al., 2013). In contrast, comparing with Wu et al. (2012) increasing temperatures cellulose-derived transformation products are reflected in more prominent peaks at 1440 cm^{-1} .

The IR spectrum of CWB reveals further signal at 1220 cm^{-1} that may corresponds to R-OH and phenol groups of biochar. During lignin charring, the substitution of methoxyl C by hydroxyl groups and formation of biphenyls occur, explaining the presence of the signal in biochar that proceed from vegetables and plants (Knicker et al., 2011). It explain the peaks for KWB and CWB samples. The typical content in lignin content in wood is about 20% to 40%, so feedstocks precedent from wood (such as biochars PWB, CWB and KWB) are expected to contain this kind of residues. However, it is not shown in the PWB biochar. This theory support the fact that PWB was produced at higher temperatures, these elevated temperatures may resulted in a complete transformation of the aromatic core of lignin. Whereas biochar KWB produced in medium conditions, which probably contain major quantities of lignin derivate compounds. It could explain, according to temperature, that increasing temperature, cellulosic and lignin compounds would reduce by decomposing, explaining why in some of these biochar this signal do not appear in the respective IR spectra (De la Rosa et al., 2014).

At the range $1075\text{-}1072\text{ cm}^{-1}$ appears a peak for two of the biochar samples, PSB and SSB respectively, attributable to C-O stretching vibration in polysaccharides (cellulose and hemicellulose). Wu et al. (2012) demonstrated that this band sustained a strong presence with increasing temperature even at 700°C . The presence of some structures in the sample such as furanose of heat-altered cellulose and hemicellulose caused this type of band. For SSB additionally, presents a high quartz content, that could cause by Si-O-Si vibrations (it also will be shown in the FESEM-data later).

At lower wavelength, below 1000 cm^{-1} the bands can be assigned out of the plane bending for CO_2^{3-} , containing for all biochars calcite. This information will be provided by SEM-data. The peak also correspond to C-H aromatic C-H ($900\text{-}650\text{ cm}^{-1}$) become more apparent with increasing temperatures (Zaho et al., 2013; Wu et al., 2012). For this reason, the wavelength rage selected for IR spectra is from $800\text{ to }4000\text{ cm}^{-1}$, explaining why some peaks do not appear in the spectra.

5.4.2. FT-IR spectra of biochars (24 months)

Respecting to biochar after 24 months (t_2) the IR spectra showed the same peaks that the initial biochar samples as it can be seen in Figure 11 at right. Comparing the IR spectra at initial time (t_0) and 24 months (t_2) at field experiment under Mediterranean climate conditions it can be concluded that there were not significate differences between each type of biochar. However, IR showed two spectra with two minimum differences in the spectra of sample PWB.

The first difference was in the PWB shown in the shoulder appearing approximately 1550 cm^{-1} , due to the graphite moieties. It indicates that there is a decrease in the degree of condensation sample when subjected to weather conditions Mediterranean. This behaviour is only shown for PWB and not seen in the other samples biochars, what suppose the loss of aromaticity of biochar with time, which could be confirmed by NMR. The second difference for the sample PWB was that peak appearing at 1050 cm^{-1} approximately which appeared in the original biochar, but after two years of exposure it became to disappear.

In general the major differences found comparing IR spectra of respincond at different times (t_0 and t_2) was a decrease reduction of aromatic peak for PWB. There were another minimal changes based on the inorganic fraction of each biochar (circa 3400 cm^{-1}) or those marked with asterisks assigned to -OH vibration due to water. So it is necessary to obtain new results of samples by other methods, demonstrating the limitation of FT-IR as technique of study for biochar study. However, FT-IR is the most used technique for the characterization and the determination of chemical composition (Hossain et al., 2011; Francioso et al., 2011).

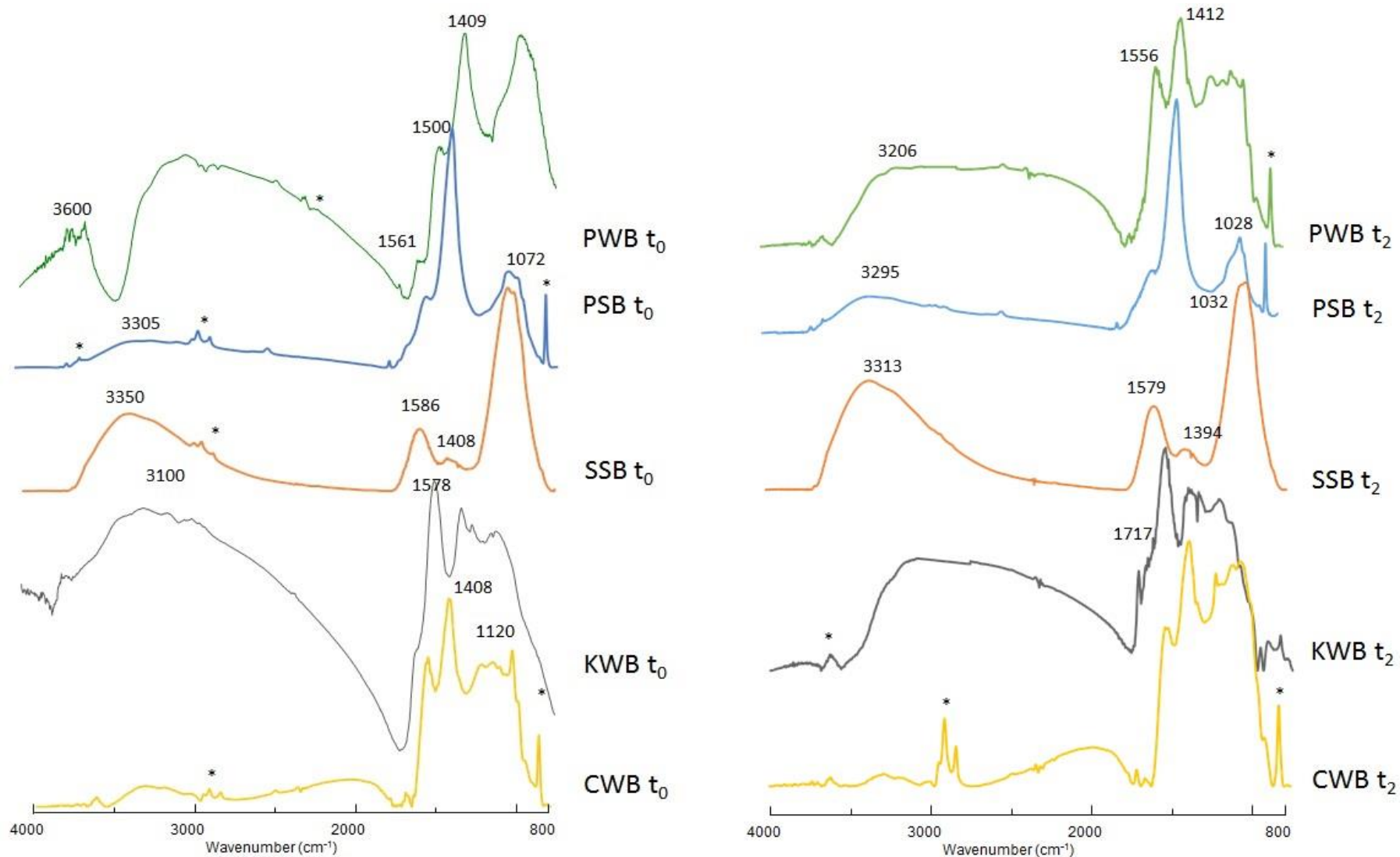


Figure 10. At left they are shown the FT-IR spectra of biochars PWB, PSB, SSB, KWB and CWB at initial time (t_0) at left; At right, it is shown the spectra of biochar PWB, PSB, SSB, KWB and CWB 24 months (t_2) after exposure at field essay in Mediterranean climate conditions. With asterisks are marked interferences signals and signals caused by H_2O and CO_2 .

5.5. ¹³C Solid-State NMR spectroscopy

Figure 11 shows the ¹³C NMR spectra for each type of biochar, while Table 8 shows the intensity distribution of the ¹³C NMR spectra obtained for the biochars PWB, PSB, SSB, KWB and CWB through time (0, 12 and 24 months at field). Due to the extremely high condensation degree of the aromatic network in PWB and CWB, the tuning of the NMR was not possible for these materials and no ¹³C NMR spectrum could be acquired. The signal appear around 1500 cm⁻¹ in the FT-IR spectra corresponding to graphitic C in these samples and its very low H/C confirm this hypothesis.

Table 8. Intensity distribution (%) of solid-state ¹³C NMR spectra of aged biochar samples of biochars at 0, 12 and 24 months. Intensity distribution was calculated after considering the effect of the spinning side bands (SSBs).

Sample	Ketone, Aldehyde 245-185 ppm	Carboxyl, Amide 185-160 ppm	Aromatic 160-100 ppm	O-alkyl 100-60 ppm	N-Alkyl, Methoxyl 60-45 ppm	Alkyl C 45-0 ppm
PWB (t ₀)	-	-	-	-	-	-
PWB (t ₁)	4	3	88	3	1	2
PWB (t ₂)	9	4	77	3	2	5
PSB (t ₀)	6	3	82	2	1	6
PSB (t ₁)	5	4	80	4	2	7
PSB (t ₂)	3	2	77	7	3	8
SSB (t ₀)	5	4	75	5	2	9
SSB (t ₁)	4	4	64	9	4	14
SSB (t ₂)	5	4	64	10	4	14
KWB (t ₀)	1	1	82	2	3	10
KWB (t ₁)	5	3	80	6	2	5
KWB (t ₂)	4	2	75	4	2	13
CWB (t ₀)	-	-	-	-	-	-
CWB (t ₁)	4	2	76	5	3	10
CWB (t ₂)	5	3	79	6	2	5

5.5.1. ¹³C NMR spectra of bulk biochars (t₀)

Concerning the ¹³C NMR spectra of the initial biochars (t₀), Aryl C (attributable to 160-90 ppm) represented for all biochars the main fraction, indicated by an intense and broad signal at 125 ppm. PSB and KWB represented the biochars with highest percentage of aryl C, over 80% of the intensity. Whereas in SSB showed the lowest value of aryl C about 75%. Presumably PWB and CWB have a greater abundance of Aryl-C. Thus the aromaticity of the biochars would be PWB ≥ CWB > KWB ≥ PSB > SSB. The higher aromaticity of PWB and CWB suggests that they were probably produced at higher pyrolysis temperature than the rest of biochars, as SSB. For instance, In that case biochar suffered less dehydration and dehydroxylation during pyrolysis transform C into aromatic structures (Knicker et al., 2008). Other authors (Zaho et al., 2013) have also reported the high presence of this kind of compounds in charcoals.

Another factor that has to be in account is the initial feedstock used for pyrolysis process, its nature will also affect the final composition of the product obtained. In the case of biochar SSB, which derived from sewage sludge, it is expected to contain large amounts of peptidous material which is cyclized but not destroyed at lower and moderate pyrolysis temperatures (Knicker, 2010), contributing to the alkyl C region of the spectrum. In this sense, it seems obvious that the contributions of N of peptides form part of the aromatic rings of heteroatoms detected in the NMR spectra. At higher temperatures of pyrolysis all alkyl C constituents are lost or transferred into aryl C.

Figure 11 shows shoulders (small peaks) in the aryl C region of biochars PSB, SSB and KWB at 151, 152 and 153, respectively. These signals may be caused by the presence of partially degraded lignin, furfurals or N-heterocyclic aromatic structures (Knicker et al., 2005). Finally, it can be concluded that biochars showed low percentages ($\leq 6\%$) in the region of carbonyl group (245-185 ppm) and in the region assigned to carboxyl/amide C group (185-160 ppm). Meanwhile, alkyl C (45-100 ppm) showed a light higher percentage (higher than 6%) for all biochars.

Finally it has to be mentioned that this last signal of alkyl C was overlapped by the spinning side bands of the aryl C signal. In order to calculate the real contribution of alkyl C groups, it was considered that these spinning side bands contributes with a comparable intensity to the total spectrum as the second spinning band between 210-180 ppm. Being the intensity of the latter subtracted from the total alkyl C region.

5.5.2. ^{13}C NMR spectra of aged Biochars (t_2)

^{13}C NMR spectra for aged biochars are showed in Figure 11, Aryl C (160-100 ppm) still represented for all biochars the main fraction of compounds, as it has been indicated in Figure 11, assigned with a signal of 125 ppm. The maximum amount of aromatic carbon are those for biochar samples PWB and PSB, explaining why it could not be possible measure the sample due to the probably reduction of carbon of biochar.

Comparing the 24-months-aged biochar (t_2) samples with those at initial time (t_0), it was observed a decrease in the aromatic region for all samples, especially for sample SSB. For the reasons discussed above, it could be said that there had been a reduction in the volatile fraction of sample PWB. The spectrum of biochar SSB showed no differences because the variation is below 5%, which could be caused by their own errors. The rest of the functional groups may be noted that were in the same proportion, except the signal belonging to the alkyl C (0-45 ppm), which was incremented in the case of biochar KWB, which is around 14%, more than double than for PSB. The different aromatic degree of biochar was attributed to pyrolysis temperature so that the abundance and extent of non-aromatic domains decrease with pyrolysis temperature. In fact, the main action was the increase of alkyl groups for the transformation of aromatic organic compounds in alkyl groups, which are reflected in the alkyl band assignment (45-0 ppm) (Table 8) for PSB (Knicker et al. 2008; Zaho et al., 2013). The same effect was observed in the samples of biochar PWB, PSB and KWB but in a lower growth.

In addition, it confirmed the results obtained by FT-IR showing whose main difference is the reduction not only the reduction of aromatic C for PWB as FT-IR predicted, NMR confirmed that fact that FT-IR could not detect for all samples. It means that biochars

may suffer a transformation from hydrophobic to hydrophilic properties including various exothermic hydration, hydrolysis and oxidation reactions involving both the ash and the condensed aromatic C components of biochar. The oxidation of biochar contributes to generate negatively charged acidic organic functional groups that contribute to CEC (Joseph et al., 2010). In fact, on timescales of hundreds of years, biochar C becomes extensively oxidized, creating groups with O functionality, which finally constitutes the most abundant C functional group after aromatic. The general trend was that the abundance of alkyl-C raises because aryl compounds (aromatic) are probably reduced by degradation. If a fraction decreases, increasing the other occurs. Degradation may aromatic ring is transformed into transformed into linear or products C-alkyls or O-alkyls (Zaho et al., 2013). In addition, biochar could have adhered soil particles with OM which could be confirmed by FESEM.

For biochar samples after 24 months of its incorporation to soil, the signal belonging to aromatic carbons (160-100 ppm) were reduced further compared with initial biochar and those aged after 12 months and further than initial biochars. Of the five types of biochar, which suffered a minor reduction in aromatic compounds is SSB. Whereupon, the aromatic C content from high to low was: CWB> PWB = PSB> KWB> SSB.

The main effect comparing initial biochar samples (t_0) with those during 24 months (t_2) was that it was more evidenced the presence of O-alkyl (100-60 ppm) and alkyl C (45-0 ppm) peaks in the NMR spectra. This suggests that some biogenic organic acids and other organic molecules on biochar surfaces become functionalized in soil environment. The most important change for biochars was that caused by SSB which in 24 months double proportion from 5% to 10%. This fact was also obtained by Laird et al., (2008) whose results suggested that aging includes both oxidation and adsorption of biogenic organic compounds. This new functionality would increase nutrient retention capacity by growing the density of surface functional groups and the adsorption of organic molecules, which contain nutrients. Consequently, biochar aged in a soil environment becomes polar and this increase WHC, nutrient residence time and, hence, the likelihood that the nutrients will be taken up by plants (Ventura et al., 2014).

However comparing the general tendency of each biochar, it can be concluded that there was high aromatic content, in agreement with elemental analysis and Van Krevelen diagram. After 24 months, there was a reduction of the aromaticity and concomitant increase of the O-alkyl/alkyl-C contributions. However there is difficult to establish a general trend because it may be particularly characteristic of each biochar were dominant as it happened. Otherwise, Kiln-wood biochar (KWB) showed an opposite trend than the others. This fact could be explained because it is more heterogeneous material than others.

An important fact to have in account is that comparing results obtained by IR spectra and by ^{13}C NMR. In the FT-IR spectra of PWB and ^{13}C NMR, the main effect experimented by samples is the reduction in aromatic compounds with time. In addition, it has been seen that the results obtained using ^{13}C MNR are more sensible to changes in the chemical composition of biochars.

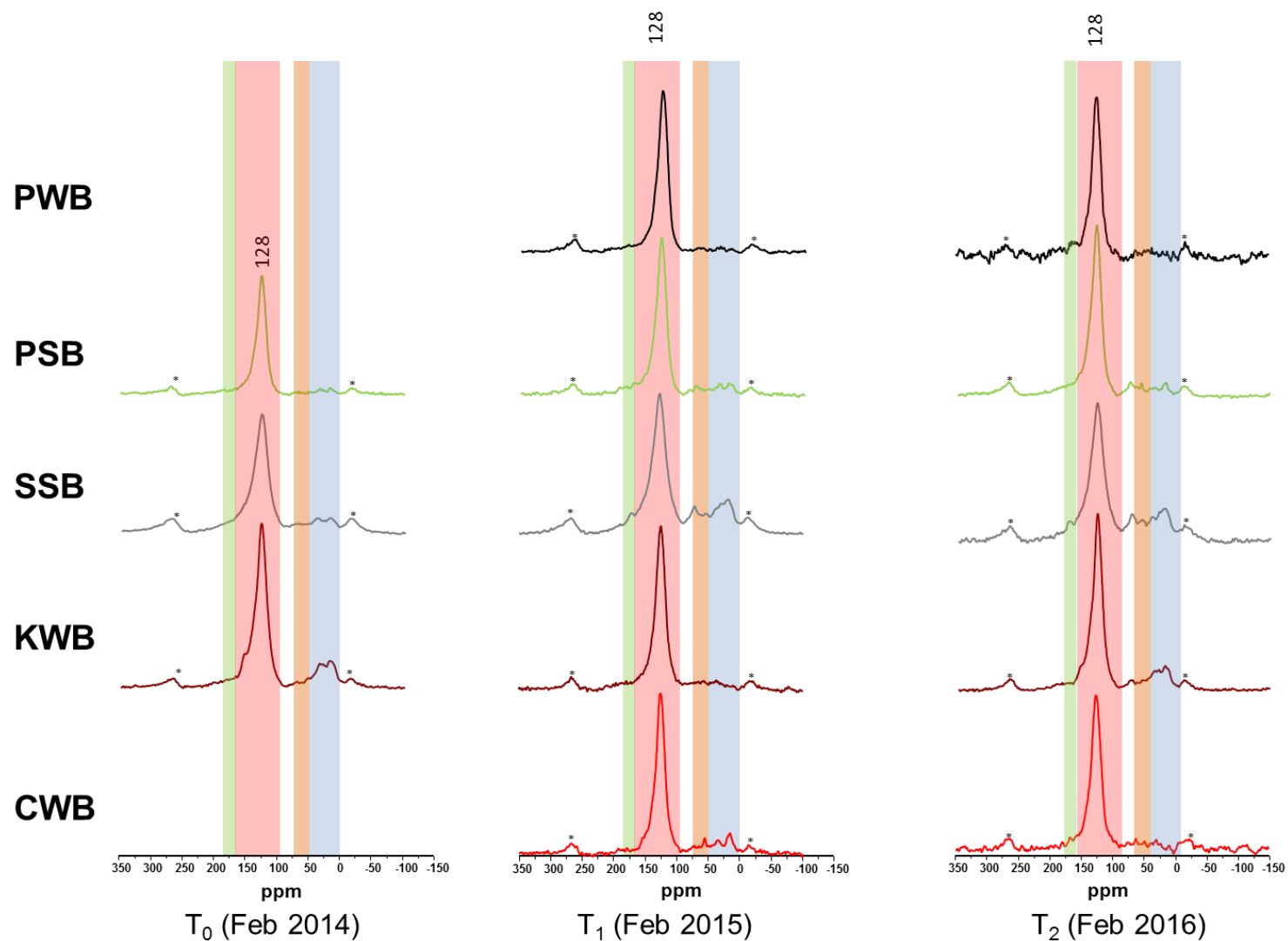


Figure 11. Solid-state ^{13}C NMR spectra of biochar PWB, PSB, SSB, KWB and CWB at initial time (February 2014, T_0), 12 months (February 2015, T_1) and 24 months (February 2016, T_2). Spinning side bands (SSBs) are marked with asterisks. In colours are indicated the different regions for the NMR spectra: green (carboxyl, amide 185-160 ppm); pink (aromatic, 160-100 ppm); white (O-alkyl, 100-60 ppm); orange (N-alkyl, methoxyl 60-45 ppm) and blue (alkyl, 45-0 ppm).

5.6. Field Emission Scanning Electronic Microscopy (FESEM)

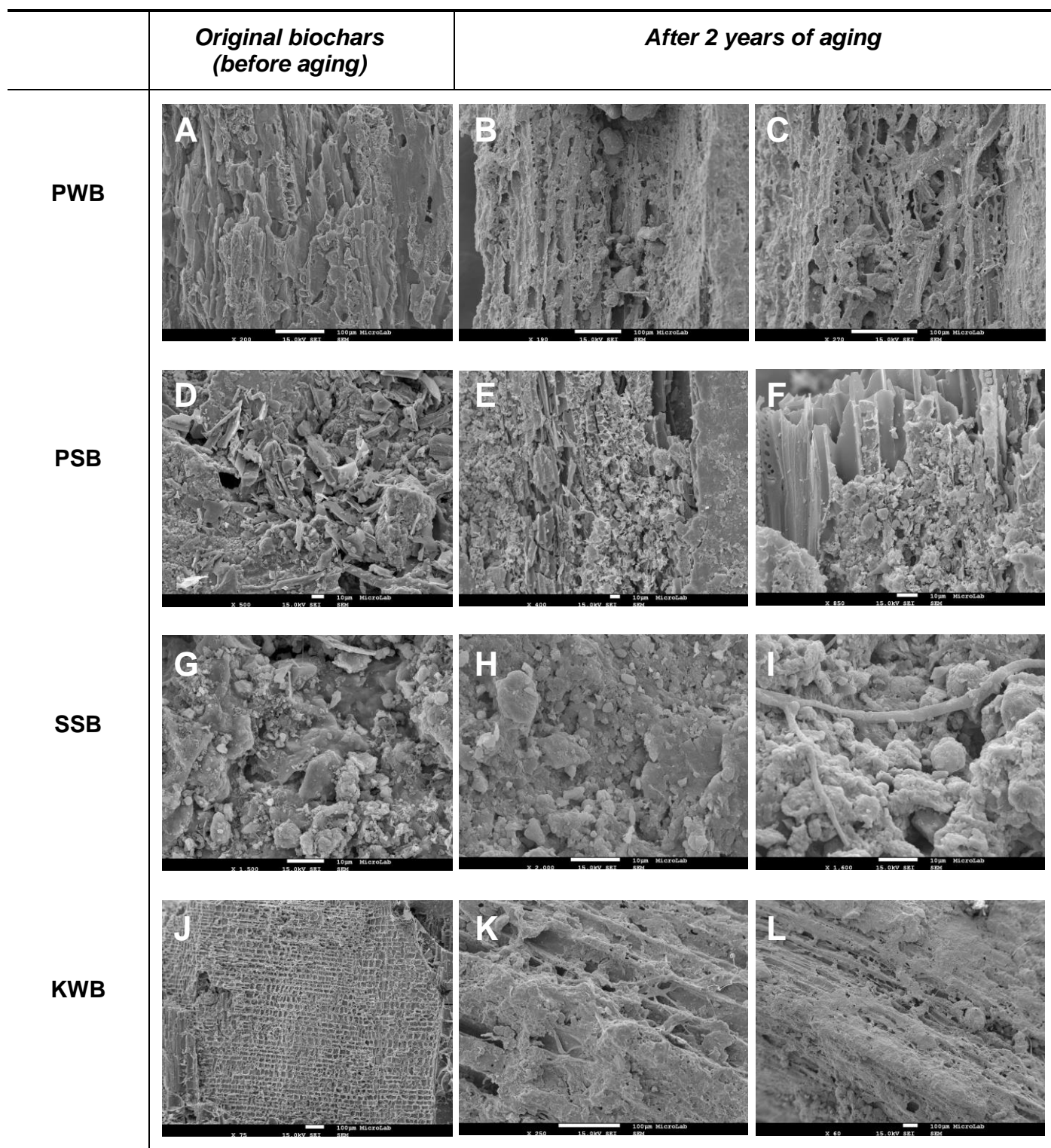


Figure 12. FESEM images of hand-picked biochar particles before (A, D, G, J) and after 2 years of aging under field conditions (B, C, E, F, H, I, K, L).

Figure 12 shows FESEM images of the biochar samples before and after 24 months of exposure under field conditions. The morphology and structure of the different biochar feedstocks are clearly observed, in particular the porous structure of the biochar samples at the initial time. The variety of the shape and size of the pores of the biochar samples

evidences that biochar structure is function of the feedstock type and pyrolysis conditions (Downie et al, 2009).

Before exposure, the original structure of the PWB biochar feedstock (i.e., wood) is observed; macropores ($>13\ \mu\text{m}$) corresponding to hollow fibers (Figure 12.A) are clearly distinguished. After 24 months of exposure, great amounts of SOM and microbial mats are observed on the biochar structure. In addition, mineral grains on and within pores and entrapped in microbial mats are noticed (Figure 12.B and 12.C).

For PSB, FESEM images revealed great amount of collapsed structures of cellulose and lignin, proceeding of the feedstock (paper sludge). Collapsed treachery elements with small pits are particularly evident (Figure 12.D). After 24 months, the same collapsed structures are clearly observed together with fine particles on their surface (Figure 12.E and 12.F).

In the case of the SSB biochar, its structure is different from the rest of the biochars studied. Due to the variety of materials that constitute sewage sludge, a great range of structures are observed, comprising a heterogeneous material. Remains of a wide range of materials are noticed: mineral grains including clay minerals, microbial mats and filaments (Figure 12.G). After 24 months, the same materials together with OM-SOM and microorganisms, such as fungal hyphae, are observed (Figure 12.H and 12.I) (De la Rosa et al., 2014).

Respecting to the initial sample of KWB, the FESEM image exhibited a good anatomical preservation of the vineyard wood feedstock, being mainly formed by macropores (Figure 12.J). After 24 months of exposure, the vineyard wood biochar is greatly coated by microbial mats and SOM, suggesting a higher affinity of this biochar for microbial colonization (Figure 12.K and 12.L). Flemming & Wingender (2014) observed that microorganisms can produce biofilms that contain aliphatic carboxyl/carbonyl, amino, amide and O-alkyl functionalities. This may be justified, considering that this biochar has the highest WHC and content of OM, as shown by De la Rosa et al. (2014). Hence, this biochar may create a suitable habitat for the development of microorganisms (Figure 12.K and 12.L). Unfortunately, it was not possible to obtain FESEM images for sample CWB.

5.7. Carbon stability of biochars (respiration experiment)

Figure 13 shows an example of the C loss, plotting the remaining C as function of the degradation time of one of the samples, specifically control sample. The respirometer analysis was made using a soil-biochar mixture after 6 months of ageing at field.

Results of the respiration experiment were achieved by using a two pool model. All the curves obtained showed coefficients of determination (R^2) greater than 0.998. Table 9 lists the proportion of the slow and fast pools of OC (A_1 , A_2) contained in biochars, their degradation constants (k_1 , k_2) and their mean residence time (MRT_1 , MRT_2). Unfortunately, it was not possible to obtain a good fitting for both replicates, so it was used only one of them.

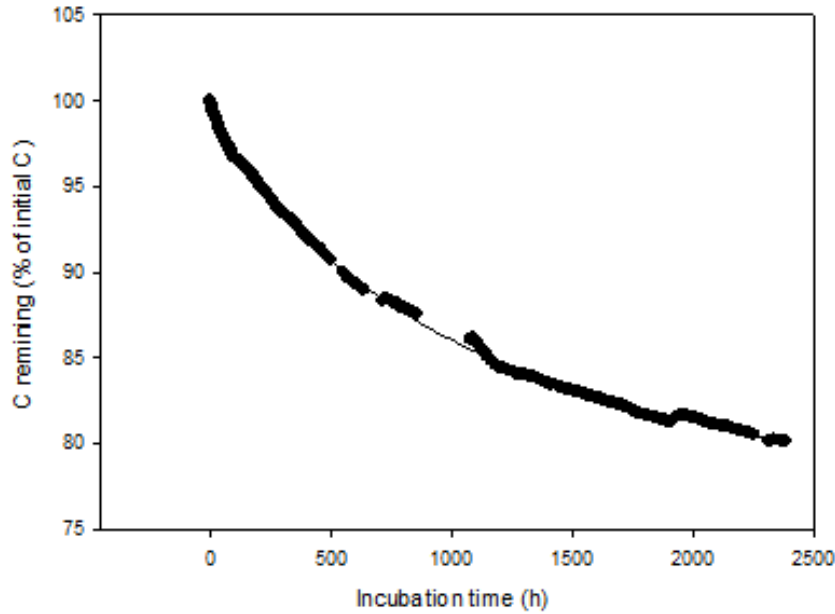


Figure 13. Example of remaining C as a function of the incubation time for control sample. For all analyzed samples, the coefficients of determination for each case (R^2) were < 0.998 . Some interruptions of data accumulation happened due to power shortages. However, the latter did affect neither the amount of CO_2 accumulation in the KOH solution nor the measured value of cumulative C loss.

Results shown are still preliminary, no distinction can be made between the mineralization of pre-existing C (from the soil substrate) before biochar amendment and the C from biochar itself. We are also conscious that the incubation conditions can not be extrapolated directly to field due to the great differences in the experimental conditions. Standard deviations were not calculated due to the existence of only one replica for each mixture of soil and biochar.

Table 9. Values of different parameters which represents the fast (A_1) and slow (A_2) OM pools, its degradation rate constants (k_1 and k_2) and their respective mean residence times (MRT_1 , MRT_2) of each biochar-soil mixtures as well as of the control. Control, soil without biochar amendment; PWB-soil mixture; PSB-soil-mixture; SSB-soil mixture; KWB-soil mixture and CWB-soil mixture.

Sample	A_1 (% of C_{org})	K_1 (years^{-1})	MRT_1 (years)	A_2 (% of C_{org})	K_2 (years^{-1})	MRT_2 (% of C_{org})	$\text{MRT}_2/\text{MRT}_1$
Control	0.7	12.3	5.7	84.1	0.12	8.7	2
PWB	2.7	11.4	0.061	97.2	0.016	43.9	720
PSB	1.4	22.8	0.044	98.6	0.099	10.1	230
SSB	12.2	35.0	0.020	87.5	0.088	7.9	400
KWB	2.4	32.4	0.031	97.3	0.016	32.4	1049
CWB	2.6	19.3	0.052	97.1	0.050	19.3	371

No differences were observed between the labile C fraction (A_1) and the stable C fraction (A_2) of bulk soil (cambisol). Thus, the ratio $\text{MRT}_2 / \text{MRT}_1$ is 2. This soil contains a relatively

high abundance of carbonates (inorganic carbon). Taking into account its low content in OC ($\leq 0.6\%$), the release of CO_2 from carbonates could mask the CO_2 released by the respiration of microorganisms. By now, this is only a preliminary hypothesis, further experiments are needed before could be onfirmed.

All biochar samples produced from wood showed comparable proportion of easily degradable OC, called as A_1 , which comprises values between 1.4% (PSB) and 2.7% (PWB). Biochar from sludge (SSB) showed the greatest presence of OC from the labile pool (12.2%). Values of A_1 are lower than those reported for the same biochars without an aging step at field (Paneque Carmona, 2014). The mean residence time of the fast pool of OM (MRT_1) ranged between 0.031 and 0.061 years. These data indicate that the labile pool is very scarce in all the biochar samples, exception SSB, and it is degraded very fast. Knicker et al (2013) reported similar MRT_1 values in fire-affected soils from Aznalcóllar. Paul and Clark (1996) published greater MRT_1 values for easily decomposable OM and plant residues.

Our results could be explained due to the metabolization of the residues from dead organisms that reimaned in the soil during drying and sample storage. Degradation of SOM is liberated and activated by rewetting and mixing. The CO_2 absorbed in soil and biochar, released after the beginning of the incubation experiment, may contribute to the fast C-loss. In addition it is possible that some biochemically labile residues formed during the thermal break down of macromolecules during pyrolysis were adsorbed within biochars. This could be available for microbial degradation, contributing to the short MRT_1 . This behaviour also has been reported during the controlled decomposition of grass chars (Hilscher et al., 2009).

Four our puroposes, the relative content of slowly-degraded OC and their mean residende time (A_2 and MRT_2) are more interesting parameters. Biochars showed elevated A_2 , ranging from 87.5 (SSB) to 98.6 % (PSB). Thus, the addition of these biochars to soil will increase the relative presence of stable C forms, being PSB and KWB the most recalcitrant biochars. Concerning the MRT_2 , which is a measure of the relative stability of the OC from those samples, PWB and KWB showed values of 43.9 and 32.4 years respectively, whereas MRT_2 of the other biochars are comparable with the soil, which are much lower than those previously reported by Kwzyakov et al. (2009).

Taking into account the data from table 9 the stability order of the biochars tested is PWB > KWB >> CWB \geq PSB \geq SSB. Of the best biochar samples to be used as tool for for carbon sequestration would be PWB and KWB, nevertheless the data are not as promising as traditionally assumed. Respiration experiment results are in agreement with results obtained by other methodologies, which have been shown in previous sections. As mentioned, PWB and KWB showed the greater microbial stability, they also have the higher percentages of carbon in the physico-chemical analysis. In addition, PWB and KWB are those also having the greatest percentage of aromaticity according to NMR. The ratio $\text{MRT}_2 / \text{MRT}_1$ can be used to compare the half life time between slow and rapid reaction carbon fraction. The $\text{MRT}_2/\text{MRT}_1$ ratio comprised from 230-1049 for biochars.

The results obtained in the experiment respirometer are in concordace with other results obtained previously (Paneque Carmona, 2014). Some studies found that short laboratory

incubation experiments resulted in great mineralization rates of OC from biochars, thus they recommended the application of longer-term studies (Luo et al., 2011; Farrell et al, 2013). Beside this, other studies have observed decreases in SOC mineralization with biochar additions (Whitman et al, 2014). Kuzyakov et al. (2009) determined that the degradation of biochar occurs in a period of hundreds or even thousands of years. On the contrary, Prayogo et al. (2014), reported no significant effect of biochar additions on native soil organic carbon. Results of our experiment indicate that the microbial degradation of the biochars tested in the calcic cambisol occurs faster than expected. Further experiments, with longer periods of incubation and including the study of the effect of the decomposition of carbonates in CO₂ emissions are needed prior achieving confident conclusions, unfortunately due to the limited time to perform this Master Thesis these experiments were not developed was not possible to perform.

6. CONCLUSIONS

The results of this work confirm the heterogeneity between biochars in which concern their physical and chemical properties (pH, conductivity, elemental composition). This is a consequence of the different nature of the feedstock and application of diverse pyrolysis conditions. Respecting to biochar alteration at field conditions under Mediterranean climate a general trend was found. In general, after 24 months, all biochars experiment a reduction in the pH (less alkaline) and conductivity. In general, OC decreased, whereas N increased slightly. The latter was attributed to the association between biochars, SOM and microbial community due to the general high porosity of biochars.

The physical fragmentation of all sorts of biochars increased significantly with time at field. FESEM analysis showed evident collapses of biochar structures after 24 months at field. FESEM analysis also showed the distribution of pores, which were consistent with the specific surface of the biochars, the visible organic mineral associations and rests of microbial activity. These results indicated that biochars are probably providing additional niches for microbiota, which would contribute to an enhancement of the soil quality from an agronomic point of view.

Comparing both spectroscopic techniques used the study the alterations in the functionality of biochars, FT-IR was not able to appreciate differences between biochar samples expoused to field experiments. However, FT-IR analyses detected changes in O-alkyl and aromatic C in all biochar samples submitted to respirometer experiment, excepting SSB. The NMR spectroscopy was able to determine more evidently the alterations in the O-alkyl, C-alkyl and C-aryl abundances of biochar samples due to ageing. In general, NMR spectra showed a reduction of aromatic-C and an increase in O-alkyl-C and alkyl-C groups when increasing the time of biochars at field.

Respiration experiments revealed that biochars PWB and KWB could enhance softly the C sequestration potential of the amended cambisol. However, the mean residence times of the supposed stable pool of C from biochars were much lower than expected. In this case, the most appropriate biochars to be used for C sequestration under Mediterranean climate conditions would be PWB and KWB, while the OC of the sample SSB are probably less stable than the bulk OM contained in the calcic cambisol used for this study. This preliminary result remarks the necessity of characterizing the biochars prior being applied to a soil for C sequestration purposes.

7. REFERENCES

- Agrafioti, E., Bouras, G., Kalderis, D., & Diamadopoulos, E. (2013). Biochar production by sewage sludge pyrolysis. *Journal of Analytical and Applied Pyrolysis*, 101, 72-78.
- Anderson T.H. and Domsch K.H., 1985. Maintenance carbon requirements of actively-metabolizing microbial populations under in situ conditions. *Soil Biology and Biochemistry*, 17, 197-203.
- Angin, D., Altintig, E., and Ennil, T., 2013. Bioresource Technology Influence of process parameters on the surface and chemical properties of activated carbon obtained from biochar by chemical activation. *Bioresource Technology*, 148, 542-549.
- Antal, M. J. 2003. The Art, Science, and Technology of Charcoal Production, 1619-1640.
- Belcher, R., Ingram, G., and Iajer, J. R. 1968. The Pyrolytic Behaviour of Organic Compounds in the Determination of Oxygen. 418-426.
- Bellantine, K., Schneider, R., Groffman, P. and Lehmann, J. 2012. Soil properties and vegetation development in four restored freshwater depressional wetlands, *Soil Science Society of America Journal*, 76, 1482-1495.
- Borchard, N., Prost, K., Kautz, T., Moeller, A. and Siemes, J. 2012a. Physical activation of biochar and its meaning for soil fertility and nutriende leaching: a greenhouse experiment. *Soil Use and Management*, 28, 177-184.
- Brewer, C.E., Hy, Y., Schmindt-Rohr, K., Loynacha, T.E., Laird, D.A. and Brown, R.C. 2012. Extent of pyrolysis impacts on fast pyrolysis biochar propierties. *Journal of Environmental Queality*, 41, 1115-1122.
- Brodowski, S., John, B., Flessa, H., and Amelung, W. 2006. Aggregate-occluded black carbon in soil. *European Journal of Soil Science*. 57, 539-546.
- Bronick, C. J., and Lal, R. 2005. Soil structure and management: a review. *Geoderma*, 124, 3-22.
- Brown, R. A., Kercher, A. K., Nguyen, T. H., Nagle, D. C., and Ball, W. P. 2006. Production and characterization of synthetic wood chars for use as surrogates for natural sorbents. *Organic geochemistry*, 37, 321-333.
- Cetin, E., Moghtaderi, B., Gupta, R., and Wall, T. F. 2004. Influence of pyrolysis conditions on the structure and gasification reactivity of biomass chars. *Fuel*, 83, 2139-2150.
- Chen, K. L., and Elimelech, M. 2006. Aggregation and deposition kinetics of fullerene (C60) nanoparticles. *Langmuir*. 22, 10994-11001.
- Chia, C. H., Gong, B., Joseph, S. D., Marjo, C. E., Munroe, P., and Rich, A. M. 2012. Imaging of mineral-enriched biochar by FTIR, Raman and SEM-EDX. *Vibrational Spectroscopy*, 62, 248- 257
- Das, O., Sarmah, A. K., and Bhattacharyya, D. 2016. Biocomposites from waste derived biochars: Mechanical, thermal, chemical, and morphological properties. *Waste Management*, 49, 560-570
- De la Rosa, J. M., and Knicker, H. 2011. Bioavailability of N released from N-rich pyrogenic organic matter: An incubation study. *Soil Biology and Biochemistry*, 43, 2368-2373.
- De la Rosa, J. M., Paneque, M., Miller, A. Z., and Knicker, H. 2014. Relating physical and chemical properties of four different biochars and their application rate to biomass production of *Lolium perenne* on a Calcic Cambisol during a pot experiment of 79 days. *Science of the Total Environment*, 499, 175-184.

- Demirbas, A. 2004. Effects of temperature and particle size on bio-char yield from pyrolysis of agricultural residues. *Journal of Analytical and Applied Pyrolysis*, 72, 243-248.
- Downie A., Crosky A. Munroe P., 2009. Physical properties of biochar, in Lehmann J., Joseph S., Biochar for environmental management: science and technology, Earthscan, United Kingdom. 13-32.
- Enders, A., Hanley, K., Whitman, T., Joseph, S., and Lehmann, J. 2012. Characterization of biochars to evaluate recalcitrance and agronomic performance. *Bioresource Technology*, 144, 644-653.
- Farrell, M., Kuhn, T. K., Macdonald, L. M., Maddern, T. M., Murphy, D. V., Hall, P. A.... Baldock, J. A. 2013. Microbial utilisation of biochar-derived carbon. *Science of the Total Environment*, 465, 288-297.
- Funke, A., and Ziegler, F. (2010). Hydrothermal carbonization of biomass: A summary and discussion of chemical mechanisms for process engineering. *Biofuels, Bioproducts and Biorefining*, 4, 160-177.
- Fu, P., Yi, W., Bai, X., Li, Z., Hu, S., and Xiang, J. 2011. Effect of temperature on gas composition and char structural features of pyrolyzed agricultural residues. *Bioresource Technology*, 120, 8211-8219.
- Francioso, O., Sanchez-Cortes, S., Bonora, S., Roldán, M. L., and Certini, G. 2011. Structural characterization of charcoal size-fractions from a burnt Pinus pinea forest by FT-IR, Raman and surface-enhanced Raman spectroscopies. *Journal of Molecular Structure*, 994, 155-162.
- Flemming, H.-C., and Wingender, J. 2010. The biofilm matrix. *Nature Publishing Group*, 8, 623-633.
- Glaser, B., and Birk, J. J. 2012. State of the scientific knowledge on properties and genesis of Anthropogenic Dark Earths in Central Amazonia (Terra Preta Indio). *Geochimica et Cosmochimica Acta*, 82, 39-51.
- Hale, S.E., Lehmann, J., Rutherford, D., Zimmerman, A.R., Bachmann, R.T., Shitumbanuma, V., O'Toole, a., Sundqvist, K.L., Arp, P.H. and Cornelissen, G. 2012. Quantifying the total and bioavailable polycyclic aromatic hydrocarbons and dioxins in biochars. *Environmental Science and Technology*, 46, 2830-2838.
- Harvey, O. R., Herbert, B. E., Rhue, R. D., and Kuo, L. J. 2011. Metal interactions at the biochar-water interface: Energetics and structure-sorption relationships elucidated by flow adsorption microcalorimetry. *Environmental Science and Technology*, 45, 5550-5556.
- Hernández-Soriano, M. C., Sevilla-Perea, A., Mingorance, M. D., and Smolders, E. 2013. Molecular Composition of Microaggregates from Artificial Soils Based on Organic Wastes and Fe-Rich Mud by FTIR Analysis. *Functions of Natural Organic Matter in Changing Environment*, 8, 1137-1141.
- Hossain, M. K., Strezov Vladimir, V., Chan, K. Y., Ziolkowski, A., and Nelson, P. F. 2011. Influence of pyrolysis temperature on production and nutrient properties of wastewater sludge biochar. *Journal of Environmental Management*, 92, 223-228.
- IEA, 2007. "IEA Bioenergy Annual Report 2006" International Energy Agency, Paris.
- IUSS Working Group WRB. 2007. World Reference Base for Soil Resources, first update 2007. *World Soil Resources Reports* 103. FAO, Rome.

- Jenkinson D.S., Powlson D.S., 1976. The effects of biocidal treatments on metabolism in soil-5. A method for measuring soil biomass. *Soil Biology and Biochemistry*. 8, 209-213.
- Jien, S. H., Wang, C. C., Lee, C. H., and Lee, T. Y. 2015. Stabilization of organic matter by biochar application in compost-amended soils with contrasting pH values and textures. *Sustainability (Switzerland)*, 7, 13319-13332.
- Jones, D. L., Rousk, J., Edwards-Jones, G., DeLuca, T. H., and Murphy, D. V. 2012. Biochar-mediated changes in soil quality and plant growth in a three-year field trial. *Soil Biology and Biochemistry*, 45, 113-124.
- Jones, J. M., Darvell, L. I., Bridgeman, T. G., Pourkashanian, M., and Williams, A. 2007. An investigation of the thermal and catalytic behaviour of potassium in biomass combustion. *Proceedings of the Combustion Institute*, 45, 113-124.
- Joseph S., Peacocke C., Lehmann J., Munroe P., 2009. 'Developing a biochar classification and test methods', in Lehmann J and Joseph S., *Biochar for environmental management: science and technology*, Earthscan, United Kingdom. 107-26.
- Joseph, S. D., Camps-Arbestain, M., Lin, Y., Munroe, P., Chia, C. H., Hook, J.... Amonette, J. E. 2010. An investigation into the reactions of biochar in soil. In *Australian Journal of Soil Research*, 48, 501-515.
- Joseph, S., Graber, E.R., Chia, C., P., Munroe, Donne, S... 2013. Shifting paradims: developments of high-efficiency biochar ferlizers base on nano-structures and soluble components. *Carbon Management*. 4, 3, 323-343.
- Kan, T., Strezov, V., and Evans, T. J. 2016. Lignocellulosic biomass pyrolysis: A review of product properties and effects of pyrolysis parameters. *Renewable and Sustainable Energy Reviews*, 57, 1126-1140.
- Keiluweit, M., Nico, P. S., Johnson, M., and Kleber, M. 2010. Dynamic molecular structure of plant biomass-derived black carbon (biochar). *Environmental Science and Technology*., 44, 1247-1253.
- Kercher, A. K., and Nagle, D. C. 2003. Microstructural evolution during charcoal carbonization by X-ray diffraction analysis. *Carbon*. 41, 15-27.
- Knicker, H., Hilscher, A., de la Rosa, J. M., González-Pérez, J. A., and González-Vila, F. J. 2013. Modification of biomarkers in pyrogenic organic matter during the initial phase of charcoal biodegradation in soils. *Geoderma*, 197-198, 43-50.
- Knicker, H. 2011. Author's personal copy N NMR spectroscopy in organic geochemistry and how spin dynamics can either aggravate or improve spectra interpretation. *Biogeochemistry*, 42, 8.
- Knicker, H. 2011. Pyrogenic organic matter in soil: Its origin and occurrence, its chemistry and survival in soil environments. *Quaternary International*, 243, 251-263.
- Knicker, H. 2010. "Black nitrogen" - an important fraction in determining the recalcitrance of charcoal. *Organic Geochemistry*, 41, 947-950
- Knicker, H. 2007. How does fire affect the nature and stability of soil organic nitrogen and carbon? A review. *Biogeochemistry*, 85, 91-118
- Knicker, H., González-Vila, F. J., and González-Vázquez, R. 2013. Biodegradability of organic matter in fire-affected mineral soils of Southern Spain. *Soil Biology and Biochemistry*, 197-198, 43-50.

- Kuzyakov, Y., Subbotina, I., Chen, H., Bogomolova, I., and Xu, X. (2009). Soil Biology and Biochemistry Black carbon decomposition and incorporation into soil microbial biomass estimated by ^{14}C labeling. *Soil Biology and Biochemistry*, 41, 210-219.
- Kwapinski, W., Byrne, C. M. P., Kryachko, E., Wolfram, P., Adley, C., Leahy, J. J.... Hayes, M. H. B. 2010. Biochar from Biomass and Waste. *Waste Biomass Valor*, 1, 177-189.
- Laird, D. A. 2008. The Charcoal Vision: A Win-Win-Win Scenario for Simultaneously Producing Bioenergy, Permanently Sequestering Carbon, while Improving Soil and Water Quality. *Biofuels*, 1, 100, 178-181.
- Lehmann, J. 2007. Bioenergy in the black. *Front. Eco. Environ*, 5, 381-387
- Lehmann, J., Rillig, M. C., Thies, J., Masiello, C. A., Hockaday, W. C., and Crowley, D. 2010. Soil Biology and Biochemistry Biochar effects on soil biota: A review. *Soil Biology and Biochemistry*, 43(9), 1812-1836.
- Lorenz, K., Preston, C. M., Krumrei, S., and Feger, K. H. 2004. Decomposition of needle/leaf litter from Scots pine, black cherry, common oak and European beech at a conurbation forest site. *European Journal of Forest Research*, 123, 177-188.
- Luo, Y., Durenkamp, M., Nobili, M. De, Lin, Q., and Brookes, P. C. 2011. Soil Biology and Biochemistry Short term soil priming effects and the mineralisation of biochar following its incorporation to soils of different pH. *Soil Biology and Biochemistry*, 43, 2304-2314.
- Lynch, J. A., Clark, J. S., and Stocks, B. J. 2004. Charcoal production, dispersal, and deposition from the Fort Providence experimental fire : interpreting fire regimes from charcoal records in boreal forests. *Can. J. For. Res.* 34, 1642-1656.
- Macías, F., and Arbestain, M. C. 2010. Soil carbon sequestration in a changing global environment. *Mitigation and Adaptation Strategies for Global Change*, 15, 511-529.
- Mao, J. D., Johnson, R. L., Lehmann, J., Olk, D. C., Neves, E. G., Thompson, M. L., and Schmidt-Rohr, K. 2012. Abundant and stable char residues in soils: Implications for soil fertility and carbon sequestration. In *Functions of Natural Organic Matter in Changing Environment*, 46, 9571-9576.
- Navia, R. and Crowley, D.E. 2010. Closing the loop on organic waste management: biochar for agricultural land application and climate change mitigation. *Waste Management and Research*, 28, 479-480.
- Nocentini, C., Certini, G., Knicker, H., Francioso, O., and Rumpel, C. 2010. Organic Geochemistry Nature and reactivity of charcoal produced and added to soil during wildfire are particle-size dependent. *Organic Geochemistry*, 41(7), 682-689.
- Nordgren, A. 1968. Short communication apparatus for the continuous, long-term monitoring of soil respiration rate in large numbers of samples. *Soil Biol*, 20(6), 955-957.
- Oh, T., Choi, B., Shinogi, Y. and Chikushi, J. 2012. Effect of pH conditions on actual and apparent fluoride adsorption by biochar in aqueous phase. *Water, Air and Soil Pollution*, 223, 3729-3738.
- Paul E.A., Clark F.E. 1996. Soil Microbiology and Biochemistry. Academic Press, Inc., San Diego.
- Paneque Carmona, M. Masther thesis, 2014. Properties of biochar used for a European ring trial (COST action: eBRN) and their impact on plant productivity and C-sequestration of a Mediterranean soil. IRNAS-CSIC. Universidad de Sevilla, 30-32.

- Pessenda, L.C.R, Gouveia, S.E.M., Aravena, R. 2001. Radiocarbon dating of total soil organic matter and humin fraction and its comparison with ^{14}C ages of fossil charcoal, *Radiocarbon Dating of Soil Organic Matter and Humin Fraction*, 43(2), 595-601.
- Pereira C.C., Pinho, C. 2014. Influence of particle fragmentation and non-sphericity on the determination of diffusive and kinetic fluidized bed biochar combustion data. *Fuel* 131, 77-88.
- Petosa, A. R., Jaisi, D. E. B. P., Quevedo, I. R., and Elimelech, M. 2010. Aggregation and Deposition of Engineered Nanomaterials in Aquatic Environments: Role of Physicochemical Interactions. *Environ. Sci. Technol.*, 44(17), 6532-6549.
- Plischke, M., and Bergersen, B. 2006. Equilibrium statistical physics (3rd edition). World scientific.
- Prayogo, C., Jones, J. E., Baeyens, J., and Bending, G. D. 2014. Impact of biochar on mineralisation of C and N from soil and willow litter and its relationship with microbial community biomass and structure. *Biol. Fertil. Soils*, 50, 695-702.
- Preston, C. M., and Schmidt, M. W. I. 2006. Black (pyrogenic) carbon : a synthesis of current knowledge and uncertainties with special consideration of boreal regions. *Biogeosciences*, 3, 397-420.
- Rajkovich, S., Enders, A., Hanley, K., Hyland, C., Zimmerman, A.R. and Lehmann, J. 2012. Corn growth and nitrogen nutrition after additions of biochar with varying properties to a temperate soil. *Biology and Fertility Soils*, 48, 271-284.
- Schmidt, M. W. I., and Noack, A. G. 2000. Black carbon in soils and sediments: Analysis, distribution, implications, and current challenges. *Global Biogeochemical Cycles*, 14(3), 777-793.
- Schimmelpfennig, S.; Glaser, B. One step forward toward characterization: Some important material properties to distinguish biochars. *J. Environ. Qual.*, 41, 1001-1013.
- Schulze, M., Mumme, J., Funke, A., and Kern, J. 2016. Geoderma Effects of selected process conditions on the stability of hydrochar in low-carbon sandy soil. *Geoderma*, 267, 137-145.
- Sevilla, M., & Fuertes, A. B. (2010). Graphitic carbon nanostructures from cellulose. *Chemical Physics Letters*, 490(1-3), 63-68.
- Six, J., Bossuyt, H., Degryze, S., and Denef, K. 2004. A history of research on the link between (micro) aggregates, soil biota, and soil organic matter dynamics. *Soil and Tillage Research*, 79, 7-31.
- Socrates, G. 2001. Infrared and RAMAN characteristic group frequencies. Tables and charts (3rd edition). John Wiley and Sons Ltd.
- Sohi, S. P., Krull, E., and Bol, R. 2010. A Review of Biochar and Its Use and Function in Soil. *Chapter 2. A Review of Biochar and its Use and Function in Soil*, 105(10), 47-82.
- Sparkes, J. 2011. Biochar : implications for agricultural productivity. Department of Agriculture, Fisheries and Forestry. Australian Government. *Technical Report 11.06* (December, 2011).
- Théry-parisot, I., Chabal, L., and Chrzavzez, J. 2010. Anthracology and taphonomy, from wood gathering to charcoal analysis. A review of the taphonomic processes modifying charcoal assemblages, in archaeological contexts. *Palaeogeography, Palaeoclimatology, Palaeoecology*, 291(1-2), 142-153.

- Vanholme, B., Desmet, T., Ronsse, F., Rabaey, K., and Breusegem, F. Van. 2013. Towards a carbon-negative sustainable bio-based economy. *Frontiers in Plant Sciences*, 4, 1-17.
- Ventura, M., Zhangb, M, E. Baldic, F. Fornasierd, G. Sorrentic, P. Panzacchic and G. Tonona. 2014. Effect of biochar addition on soil respiration partitioning and root dynamics in an apple orchard. *European Journal of Soil Science*, 65, 186-195.
- Watzinger, A., Feichtmair, S., Kitzler, B., Zehetner, F., Kloss, S., Wimmer, B.... Soja, G. 2014. Soil microbial communities responded to biochar application in temperate soils and slowly metabolized ¹³C-labelled biochar as revealed by ¹³C PLFA analyses: Results from a short-term incubation and pot experiment. *European Journal of Soil Science*, 65, 40-51.
- Whitman, T., Enders, A., and Lehmann, J. 2014. Soil Biology and Biochemistry Pyrogenic carbon additions to soil counteract positive priming of soil carbon mineralization by plants. *Soil Biology and Biochemistry*, 73, 33-41.
- Whitman, T., Scholz, S. M., and Lehmann, J. 2010. Biochar projects for mitigating climate change : an investigation of critical methodology issues for carbon accounting. *Carbon Management*, 1(1), 89-107.
- Wilson M.A. 1987. NMR Techniques and Applications in Geochemistry and Soil Chemistry. Pergamon Press, Oxford.
- Wu, W., Yang, M., Feng, Q., Mcgrouter, K., Wang, H., Lu, H., and Chen, Y. 2012. Chemical characterization of rice straw-derived biochar for soil amendment. *Biomass and Bioenergy*, 47, 268-276. Wu, Y., Xu, G., and Shao, H. B. 2014. Furfural and its biochar improve the general properties of a saline soil. *Solid Earth*, 5(2), 665-671.
- Zhao, X., Ouyang, W., Hao, F., Lin, C., Wang, F., Han, S., and Geng, X. 2013. Bioresource Technology Properties comparison of biochars from corn straw with different pretreatment and sorption behaviour of atrazine. *Bioresource Technology*, 147, 338-344.
- Zhao, L., and Cao, X. 2013. Heterogeneity of biochar properties as a function of feedstock sources and production temperatures. *Journal of Hazards Materials*, 257, 1-9.
- Zielińska, A., and Oleszczuk, P. 2015. The conversion of sewage sludge into biochar reduces polycyclic aromatic hydrocarbon content and ecotoxicity but increases trace metal content. *Biomass and Bioenergy*, 75, 235-244.